

**Dear Dr. Blume and reviewers:**

**Thank you very much for your comments on our manuscript again. We have made correction or given explanations in response to your comments. Please see below our responses in blue to all your comments. The marked-up version is also attached following the responses to the comments.**

**Sincerely,**

**Wei Hu**

**Bing Cheng Si**

.....

Comments to the Author:

Dear authors,

both referees recommend publication and we will be able to proceed as soon as the minor revisions as suggested by the referees and myself have been implemented.

One of the referees suggests focusing on the introduction of the TA model at the Canadian site, including the comparison to the SA model and the discussion of correlations between site factors and TA model components and not including the comparison to the sites in China and Italy. I suggest to keep the inter-site comparison (and to keep it short), but I agree with the referee that these datasets need to be introduced (shortly) in the methods section. To avoid confusion it also needs to be made clear in methods, results and discussion what the purpose of this inter-site comparison is (by adding half a sentence with this information at the corresponding locations in the text).

Please also see some additional comments in the attached pdf document.

Best regards,

Theresa Blume

**Response:**

**Many thanks for your handling our manuscript.**

**As you suggested, we keep the inter-site comparison in short. We think the inter-site comparison is necessary for illustrating when the new model outperforms the old one in terms of estimation of spatially distributed soil water content (SWC). As demonstrated in this study, the new method outperforms the old one at small scales, but does not at large scales like for the Italian site. The reasons are given in lines 551-572.**

The introduction of the datasets from the Chinese site and Italian site was moved in the method section (Lines 163-171). The purpose of inter-site comparison was also illustrated at Lines 17169-176: "**With these two datasets, spatially distributed SWC was estimated using the two different decomposition methods. Performances in estimation of spatially distributed SWC were compared among all three sites to further demonstrate conditions under which the new decomposition outperformed the method suggested by Perry and Niemann (2007).**"

Comments from the attached PDF file

L28-29: please correct/rephrase this sentence

Response:

We have changed it to "The TA model can be used to construct a high-resolution distribution of SWC at small watershed scales from coarse-resolution remotely sensed SWC product."

L40: change "thick" to "in depth"

Response:

Yes, revised.

L154: shortly introduce the two other data sets/ research sites here and explain the purpose of the comparison.

Response:

Yes, as we stated above, we have made a revision at Lines 163-176.

L272: isn't this the basic split sample approach?

As far as I understand external validation would employ a different type of data set for validation, not just a different time period.

Response:

Yes, it is split sample validation. We changed the external validation to split sample validation throughout the manuscript.

L310: please make sure to give clear indication to which figure you are referring to in which statement.

Response:

Yes, done.

L321: indicate which figure you are referring to

Response:

Yes, done. it is Fig. 3a.

L346: Indicate which figure you are referring to here.

Response:

Yes, done. it is Fig. 3b.

L351-353: discussion?

Response:

Yes, it belongs to discussion. We moved and reorganized in the discussion at lines L531-L538.

**" Therefore, the influence of depth to CaCO<sub>3</sub> layer and SOC partially reflected the role of topography in driving snowmelt runoff along slopes in the spring, which contributes to increasing water recharge in depressions. As already demonstrated, topographically lower positions corresponded to more negative  $R_m$  during the dry periods. This implies that depressions lost more water during discharge. This is because depressions usually corresponded to vegetation with a larger leaf area index, which would result in higher evapotranspiration and more water loss during discharge periods. "**

L389: hypotheses can generally only be rejected (maybe your findings can support a hypothesis, but I would be careful with the wording of "accepting a hypothesis")

Response:

We changed it to "**our hypothesis that underlying spatial patterns exist in the  $R_m$  was supported**".

L431-434: indicate where we can see this in the presented data.  
Might also fit better in to the discussion than into the results section.

Response:

The poor performance on October 27, 2009 can be seen from Fig. 7a. This was added at Line 449. For all three dates, the poor performance can be seen from the NSCE values shown in Fig. 8a. As you suggested, this may fit better in the discussion. We combine this comments and the one below, we discussed the reasons why the performance on these three dates are not satisfactory at Lines 622-628: "**The  $\sigma_{\hat{n}}^2(M_{in})$  was greater than the  $\sigma_{\hat{n}}^2(R_m)$  (Fig. 5), indicating that time stability was more important than time instability for SWC estimation. For the three dates in the fall (i.e., October 22, 2008, August 27, 2009, and October 27, 2009), strong evapotranspiration and deep drainage in depressions resulted in a much lower SWC at the near surface than in the spring. This resulted in reduced time stability of SWC pattern and poor performance of both models and validation methods in terms of SWC evaluation (Fig. 8a).**"

L445: add a sentence or two to the discussion on why this is the case (possibly jointly for cross-validation and split sample validation).

Response:

Please see the comments above.

L470-474: move this to Methods

Response:

Yes, done.

L489-492: move this to Methods

Response:

Yes, done.

L598-601: rephrase - not clear/convincing

Response:

The previous sentence may be confusing, and we believe that if the quality of the two models are the same, the SA model should be used considering that it is simpler. So, we changed this discussion to "**On the contrary, when underlying spatial patterns do not exist in the  $R_m$  or the  $R_m$  has negligible variances, the SA model may be selected although these two models yield the same quality of SWC estimation. This is because the TA model needs one more spatial parameter (i.e.,  $M_{\hat{m}}$ ) than the SA model.**"

L609: do you mean deeper? or soil layers extending from the surface to greater depth? please clarify.

Response:

We mean the latter. We changed it to "**SWC evaluation was more accurate for soil layers extending from the surface to greater depths.**"

L632: in-situ?

Response:

Yes, we changed it to "in situ SWC".

L633: change "remote sensed SWC" to "remotely sensed SWC"

Response:

Yes, done.

L634: what do you mean here? in-situ measurements? change "the future study" to "future research"

Response:

Yes, we changed it to "**in situ SWC measurements**". "the future study" was changed to "**future research**".

L635: rephrase  
(do you mean conduct?)

Response:

Yes, we mean conduct. We changed it to "**future research should be conducted to estimate...**".

L638: rephrase

Response:

This sentence was moved to the discussion part at Lines 612-616: "**On the contrary, when underlying spatial patterns does not exist in the  $R_m$  or the  $R_m$  has negligible variances, the SA model may be selected although these two models yield the same quality of SWC estimation. This is because the TA model needs one more spatial parameter (i.e.,  $M_{\hat{m}}$ ) than the SA model.**"

Fig.3: the corresponding dates for each number are too small to read properly.

Response:

Yes, we revised.

Fig.8: please indicate the dates in the plot and give the NSCE values in the caption.

Response:

Yes, done.

Fig.9: difference between what? this information is missing in the caption and only shows up in the y-axis label.

Response:

We changed the caption as "**Nash-Sutcliffe coefficient of efficiency (NSCE) difference between the TA and SA models in terms of soil water content estimation using both cross validation (CV) and split sample validation (SV) as a function of space-invariant temporal anomaly  $A_{i\hat{n}}$  for (a) 0–0.2 and (b) 0–1.0 m.**"

Fig.10: difference between what? See previous comment.

please add the NSCE values themselves on the second y axis. Markers can be small compared to the ones indicating the differences.

Response:

We changed the caption as "**Nash-Sutcliffe coefficient of efficiency (NSCE) difference between the TA and SA models in terms of soil water content estimation using cross validation as a function of space-invariant temporal anomaly  $A_{i\hat{n}}$  for (a) 0–0.06 m of the Chinese Loess Plateau hillslope and (b) 0–0.15 m of the GENCAI network in Italy. The NSCE values for both models are also shown.**"

The NSCE values themselves are shown on the second y axis.

Comments from Reviewer 1#

Major comment

The authors have made a thorough job during the revision of their manuscript according to the reviewers comments. I however do not agree with the authors comply to the second reviewer's request of including additional datasets into their study while at the same time maintaining the overall structure of the manuscript. As it is now, the manuscript targets both, a benchmarking of the new model against two additional datasets and a correlation analysis between model components and site factors at the Canadian site.

The problem is that the correlations are only discussed for the Canadian site whereas the two other sites are only very superficially introduced and discussed. I think introducing and discussing also the two other sites in similar detail like the Canadian site would make the manuscript too lengthy and complicated.

The manuscript would gain considerably if the authors would focus on either one of the two aims.

I personally recommend focusing on the introduction of the TA model at the Canadian site, including the comparison to the SA model and the discussion of correlations between site factors and TA model components.

An alternative would be introducing all three sites properly in the material and methods section and focus on a model benchmarking of TA and SA models. At the same time a discussion of correlations between site factors and model components at the Canadian site should be skipped.

I find that the manuscript is otherwise publishable, apart from some minor technical details. I therefore recommend another round of minor revisions.

Response:

Many thanks for your comments again.

Regarding the major concern you raised, we agree more with the Editor Dr. Blume. We would focus mainly on the dataset from the Canadian site. But at the same time, the datasets from other two sites are also briefly introduced, and the inter-site comparison of the performance of the models was made for further demonstrating under which condition the new model outperforms the old one in terms of estimation of spatially distributed soil water content (SWC).

Minor comments:

L71: equals or corresponds to ?

Response:

It should be "equals" because we mean that the spatial variance in the temporal anomaly is identical to the spatial variance of the space-variant term in the temporal anomaly.



L122: Materials and methods: If the authors wish to keep the application of the models to the two other sites they should also be presented in similar detail as the Canadian site in the materials and methods section (see major comment).

Response:

As suggested by the Editor, the introduction of these two sites was listed in the methods part, and the purpose of inter-site comparison was also added.

L217: maybe better: "the spatial variance"

Response:

Yes, we agree that the variance indicates spatial variance. But as we already mentioned before at Lines 187-188: "**the variance or covariance denotes the quantity in space without specifications**". Therefore, the "spatial" may be omitted here.

L243: I think "contribution" is not the correct term here (see comment below)

Response:

Yes, we avoided the use of "contribution" throughout the manuscript. Instead, we used "account for" or just simply remove the "contribution" from "percentage contribution".

L256: The  $A_{tn}$  looks strange..

Response:

Yes, revised.

L321: of the original SWC

Response:

Yes, done.

L363: I do not agree that something can contribute with more than 100% to another thing.  $\sigma^2(M_{tn})$  merely takes on such large values because it is countered by a negative covariance. I therefore suggest to avoid using the term "contributes" in this context (throughout the entire manuscript). I apologize for not having pointed this out in the first review. Since the percentages of the variance are not bounded by 100% the authors should rather contrast it with the contribution of the other positive component in equation 8. Otherwise it is unclear whether

the contribution was really high or not. It occurred to me at this point that including a shrinkage regularization in the model fitting may be interesting in future studies.

Response:

Yes, we agree with your comments. The reason we use the term "contributes" was that previous studies (Mittelbach and Seneviratne, 2012; Brocca et al., 2014; Rötzer et al., 2015) did the same way. To avoid confusion, we did not use this term anymore. In addition, thanks for your good suggestions on "a shrinkage regularization in the model fitting" in future studies.

L421 maybe better: "..validation methods. This is also supported by the increasing AICc.."

Response:

Yes, we changed it to "**validation methods. This is also supported by the increasing AICc values with the increasing number of parameters resulting from more EOFs (data not shown).**" (lines 441-443).

L542: just to make it easier for the reader to follow the manuscript: stable in time or in space?

Response:

It's stable in time. So, we changed it to "stable in time".

Comments from Reviewer 2#

The authors successfully addressed the reviewers' comments. Specifically, the methodology was clarified and the addition of two datasets makes the results more significant and robust. Therefore, I suggest the paper can be accepted as is.

Response:

Thank you for reviewing our manuscript again and your approval of this manuscript.

1 Estimating spatially distributed soil water content at small watershed  
2 scales based on decomposition of temporal anomaly and time stability  
3 analysis

4 Wei Hu<sup>2</sup> and Bingcheng Si<sup>1,2</sup>

5 <sup>1</sup>College of Hydraulic and Architectural Engineering, Northwest A&F University, Yangling,

6 712100, -China

7 <sup>2</sup>University of Saskatchewan, Department of Soil Science, Saskatoon, SK S7N 5A8, Canada

8 Correspondence to: Bingcheng Si (bing.si@usask.ca)

Formatted: Superscript

Formatted: Font: Not Italic, Superscript

Formatted: Font: Not Italic

Formatted: Font: Not Italic

Formatted: Font: Not Italic, English (Canada)

Formatted: Font: Not Italic, Superscript

Formatted: Font: Not Italic

Formatted: Font: Not Italic, English (Canada)

9 **Abstract**

10 Soil water content (SWC) is crucial to rainfall-runoff response at the watershed scale.  
11 A model was used to decompose the spatiotemporal SWC into a time-stable pattern  
12 (i.e., temporal mean), a space-invariant temporal anomaly, and a space-variant  
13 temporal anomaly. The space-variant temporal anomaly was further decomposed  
14 using the empirical orthogonal function (EOF) for estimating spatially distributed  
15 SWC. This model was compared to a previous model that decomposes the  
16 spatiotemporal SWC into a spatial mean and a spatial anomaly, with the latter being  
17 further decomposed using the EOF. These two models are termed temporal anomaly  
18 (TA) model and spatial anomaly (SA) model, respectively. We aimed to test the  
19 hypothesis that underlying (i.e., time-invariant) spatial patterns exist in the  
20 space-variant temporal anomaly at the small watershed scale, and to examine the  
21 advantages of the TA model over the SA model in terms of the estimation of spatially

22 distributed SWC. For this purpose, a dataset of near surface (0–0.2 m) and root zone  
23 (0–1.0 m) SWC, at a small watershed scale in the Canadian prairies, was analyzed.  
24 Results showed that underlying spatial patterns exist in the space-variant temporal  
25 anomaly because of the permanent controls of “static” factors such as depth to the  
26 CaCO<sub>3</sub> layer and organic carbon content. Combined with time stability analysis, the  
27 TA model improved the estimation of spatially distributed SWC over the SA model,  
28 especially for dry conditions. Further application of these two models demonstrated  
29 that the TA model outperformed the SA model at a hillslope in the Chinese Loess  
30 Plateau, but the performance of these two models in the GENCAI network (~250 km<sup>2</sup>)  
31 in Italy was equivalent. The TA model ~~has potential~~can be used to construct a  
32 ~~spatially distributed~~high-resolution distribution of SWC at small watershed scales  
33 from coarse-resolution remotely sensed SWC product.

34 Keywords: Soil moisture; Soil water downscaling; Empirical orthogonal function;  
35 Statistical models; Time stability

## 36 1. Introduction

37 Soil water content (SWC) of surface soils exerts a major influence on a series of  
38 hydrological processes such as runoff and infiltration (Famiglietti et al., 1998;  
39 Vereecken et al., 2007; She et al., 2013a). Soil water content in the root zone is, in  
40 many cases, linked to vegetative growth (Wang et al., 2012; Ward et al., 2012; Jia and  
41 Shao, 2013). Obtaining accurate information on the spatiotemporal SWC is crucial for  
42 improving hydrological prediction and soil water management (Venkatesh et al., 2011;

43 Champagne et al., 2012; She et al., 2013b; Zhao et al., 2013). While remote sensing  
44 has advanced SWC measurements of surface soils (<5 cm ~~thick~~ in depth) at basin  
45 (2,500–25,000 km<sup>2</sup>) and continental scales (Robinson et al., 2008), characterization of  
46 spatially distributed SWC at small watershed (0.1–80 km<sup>2</sup>) scales still poses a  
47 challenge. A method is needed for estimating spatially distributed SWC in the near  
48 surface and root zone at watershed scales.

49 Time stability of SWC, which refers to similar spatial patterns of SWC across  
50 different measurement times (Vachaud et al., 1985; Brocca et al., 2009), has been used  
51 for estimating spatially distributed SWC (Starr, 2005; Perry and Niemann, 2007;  
52 Blöschl et al., 2009). This method is conceptually appealing, but assumes completely  
53 time-stable spatial patterns of SWC.

54 The time-stable pattern does not explain all of the spatial variances in SWC,  
55 indicating the existence of time-variant components (Starr, 2005). In order to identify  
56 underlying patterns of SWC that have time-variant components, the spatiotemporal  
57 SWC was decomposed into a spatial mean and a spatial anomaly. The spatial anomaly  
58 of the SWC was further decomposed into the sum of the product of time-invariant  
59 spatial patterns (EOFs) and temporally varying, but spatially constant coefficients  
60 (ECs) using the empirical orthogonal function (EOF) (Fig. 1) (Jawson and Niemann,  
61 2007; Perry and Niemann, 2007, 2008; Joshi and Mohanty, 2010; Korres et al., 2010;  
62 Busch et al., 2012). Spatially distributed SWC estimates based on the decomposition  
63 of spatial anomaly outperformed those based on time-stable patterns (Perry and  
64 Niemann, 2007).

65 Recently, the spatiotemporal SWC was also decomposed into a temporal mean and  
66 a temporal anomaly (Mittelbach and Seneviratne, 2012) (Fig. 1). Previous studies  
67 indicated that the contribution of the temporal anomaly to the total spatial variance  
68 was notable (Mittelbach and Seneviratne, 2012; Brocca et al., 2014; Rötzer et al.,  
69 2015). These studies, however, only focused on surface soils at large scales ( $> 250$   
70  $\text{km}^2$ ). Vanderlinden et al. (2012) suggested that the temporal mean may be further  
71 decomposed into its spatial mean and residuals, and the temporal anomaly may be  
72 further decomposed into space-invariant term (i.e., spatial mean of temporal anomaly)  
73 and space-variant term (i.e., spatial residuals of temporal anomaly) (Fig. 1). Note that  
74 the spatial variance in the temporal anomaly (Mittelbach and Seneviratne, 2012)  
75 equals that of the space-variant term of the temporal anomaly (Vanderlinden et al.,  
76 2012). The further decomposition of the temporal anomaly may be physically  
77 meaningful, because the space-invariant and space-variant terms in the temporal  
78 anomaly may be forced differently. However, the models of Mittelbach and  
79 Seneviratne (2012) and Vanderlinden et al. (2012) have not been used for estimating  
80 spatially distributed SWC. If the space-variant terms are ignored during the estimation  
81 of spatially distributed SWC, their models are equivalent to that based on time-stable  
82 patterns. Therefore, estimation of spatially distributed SWC may be improved by  
83 incorporating the space-variant term of the temporal anomaly if underlying (i.e.,  
84 time-invariant) spatial patterns exist in the temporal anomaly.

85 To our knowledge, the importance of the space-variant term of the temporal  
86 anomaly and its physical meaning at small watershed scales is not well-known. Based

87 on previous studies (Perry and Niemann, 2007; Mittelbach and Seneviratne, 2012;  
88 Vanderlinden et al., 2012), we assume soil water dynamics at watershed scales can be  
89 decomposed into three components (Fig. 1): (1) time-stable pattern (i.e., temporal  
90 mean, spatial forcing): the “static” factors such as soil and topography control the  
91 pattern; (2) space-invariant temporal anomaly (temporal forcing): the “dynamic”  
92 factors such as meteorological variables and vegetation change with time, and  
93 therefore modify SWC in time, regardless of spatial locations; and (3) space-variant  
94 temporal anomaly (interactions between spatial forcing and temporal forcing): this  
95 term represents interactions between “static” and “dynamic” factors. For example,  
96 SWC recharge introduced by a rainfall may be modified by topography through  
97 runoff processes; SWC loss triggered by evapotranspiration may be regulated by  
98 topography through solar radiation exposure.

99 The “static” factors may be persistent in the space-variant temporal anomaly, and  
100 their impacts on the space-variant temporal anomaly likely change with time. Thus,  
101 we hypothesize that some underlying (i.e., time-invariant) spatial patterns exist in the  
102 space-variant temporal anomaly, and their impacts can be modulated by a time  
103 coefficient, both of which can be obtained by the EOF method (Fig. 1). If the  
104 hypothesis is true, the estimation of spatially distributed SWC utilizing the EOF  
105 decomposition may outperform the one suggested by Perry and Niemann (2007). This  
106 is because: (1) the spatial anomaly which was decomposed using the EOF in Perry  
107 and Niemann (2007) lumped the time-stable pattern and space-variant temporal  
108 anomaly together (Fig. 1); (2) the underlying spatial patterns in the spatial anomaly

109 may not fully capture both time-stable patterns and patterns in the space-variant  
110 temporal anomaly due to the possible nonlinear relations between these two terms.

111 Therefore, the objectives were (1) to test the hypothesis that underlying spatial  
112 patterns exist in the space-variant temporal anomaly at small watershed scales and (2)  
113 to examine whether the decomposition of the space-variant temporal anomaly using  
114 the EOF has any advantages over the decomposition of the spatial anomaly (Perry and  
115 Niemann, 2007) for estimating spatially distributed SWC. Two steps were included in  
116 the estimation of spatially distributed SWC. First, the spatial mean SWC was upscaled  
117 from the SWC measurement at the most time-stable location using time stability  
118 analysis. Following this, the spatially distributed SWC was downscaled from the  
119 estimated spatial mean SWC. For the purpose of this study, spatiotemporal SWC  
120 datasets at depths of near surface (0–0.2 m) and root zone (0–1.0 m) from a Canadian  
121 prairie landscape were used. Spatiotemporal SWC of samples taken 0–0.06 m from a  
122 hillslope (100 m) in the Chinese Loess Plateau and 0–0.15 m from the GENCAI  
123 network (~250 km<sup>2</sup>) in Italy were also used to further demonstrate conditions under  
124 which the decomposition of the spatial anomaly was beneficial to the estimation of  
125 spatially distributed SWC.

## 126 2. Materials and methods

### 127 2.1 Study area and data collection

128 This study was mainly conducted in the Canadian prairie pothole region (hereafter  
129 abbreviated as Canadian site) at St. Denis National Wildlife Area (52°12' N, 106°50'

Formatted: Heading 2, Indent: First line: 0 ch



130 W) with an area of 3.6 km<sup>2</sup>. This area has a humid continental climate (Peel et al.,  
131 2007), and had a mean annual air temperature of 1.9 °C and a mean annual  
132 precipitation of 402 mm during the study period (Fig. 2). A variety of depressions,  
133 knolls, and knobs result in a sequence of undulating slopes (Biswas et al., 2011). The  
134 elevation varies from 554.8 to 557.5 m. The soils are dominated by clay loam textured  
135 Mollisols (Soil Survey Staff, 2010) and covered by mixed grass, i.e., smooth brome  
136 grass (*Bromus inermis*) and alfalfa (*Medicago sativa* L.). The near surface soil  
137 porosity ranges from 38% (knolls) to 70% (depressions). Calcium carbonates (CaCO<sub>3</sub>)  
138 derived mostly from fragments of limestone rocks are common in the Canadian  
139 Prairies. The CaCO<sub>3</sub> is dissolved by the slightly acidic rainwater moving through the  
140 upper horizons and deposited to lower horizons. The heterogeneous amount of  
141 infiltrated water resulted in a varying depth of CaCO<sub>3</sub> layer ranging from almost 0 m  
142 in the knolls to 2.1 m in the depressions. A 576 m long sampling transect with 128  
143 sampling locations spaced at 4.5 m intervals was established over several rounded  
144 knolls and depressions. At each location, a time domain reflectometry probe was used  
145 to measure SWC of the near surface soil (0–0.2 m), and a neutron probe was used to  
146 collect SWC measurements at 0.2 m intervals between a depth of 0.2 and 1.0 m. The  
147 SWC was measured on a volumetric basis and expressed as a percentage (%) volume  
148 of water per unit soil volume. The SWC of the root zone was calculated by averaging  
149 the SWC of 0–0.2, 0.2–0.4, 0.4–0.6, 0.6–0.8, and 0.8–1.0 m. Soil water content was  
150 measured on 23 dates from July 17, 2007 to September 29, 2011. The SWC dataset  
151 was collected in all seasons except winter, and accurately portrays the variations in

152 soil water conditions in the study area. In addition to the SWC dataset, the soil,  
153 vegetative, and topographical properties were obtained at each sampling location.  
154 These properties included soil particle components (clay, silt, and sand contents), bulk  
155 density, soil organic carbon (SOC) content for the surface layer, A horizon depth, C  
156 horizon depth, depth to the CaCO<sub>3</sub> layer, leaf area index, elevation, cos(aspect), slope,  
157 curvature, gradient, upslope length, solar radiation, specific contributing area,  
158 convergence index, wetness index, and flow connectivity. Detailed information on the  
159 measurements can be found in Biswas et al. (2012). The datasets from the Canadian  
160 site were used to demonstrate the following two aspects in detail: (1) different  
161 components of spatiotemporal SWC and their contributing factors, and (2) the  
162 advantages of the new decomposition method over the method suggested by Perry and  
163 Niemann (2007) in terms of the estimation of spatially distributed SWC.

164 Besides the Canadian site, datasets from a hillslope scale in a Chinese site and a  
165 large watershed scale in a Italian site were applied. Along a hillslope of 100 m in  
166 length in the Chinese Loess Plateau, SWC of 0–0.06 m was measured 136 times from  
167 June 25, 2007 to August 30, 2008 by a Delta-T Devices Theta probe (ML2x) at 51  
168 locations (Hu et al., 2011). The hillslope was covered by *Stipa bungeana* Trin. and  
169 *Medicago sativa* L. in sandy loam and silt loam soils. In the GENCAI network (~250  
170 km<sup>2</sup>) in Italy, SWC of 0–0.15 m was measured by a TDR probe at 46 locations, 34  
171 times from February to December in 2009 (Brocca et al., 2012, 2013). The GENCAI  
172 area was dominated by grassland with a flat topography, in silty clay soils. With these  
173 two datasets, spatially distributed SWC was estimated using the two different

174 decomposition methods. Performances in estimation of spatially distributed SWC  
175 were compared among all three sites to further demonstrate conditions under which  
176 the new decomposition outperformed the method suggested by Perry and Niemann  
177 (2007).

## 178 2.2 Statistical models for decomposing soil water content

179 Spatiotemporal SWC at small watershed scales was decomposed into three  
180 components: time-stable pattern, space-invariant temporal anomaly, and space-variant  
181 temporal anomaly. This model was compared to the one that decomposed SWC into  
182 spatial mean and spatial anomaly (Perry and Niemann, 2007). Both the space-variant  
183 temporal anomaly and spatial anomaly were decomposed using the EOF method. The  
184 two models are termed temporal anomaly (TA) model and spatial anomaly (SA)  
185 model, respectively. Figure 1 displays the differences between the two models. Each  
186 component will be explained in detail later. The explanation of nomenclatures is listed  
187 in Table A1. Because we focus on estimating spatial distribution of SWC at any given  
188 time, only spatial variances of SWC were taken into account. Therefore, the variance  
189 or covariance denotes the quantity in space without specifications.

### 190 2.2.1 The SA model

191 Perry and Niemann (2007) expressed SWC at location  $n$  and time  $t$  ( $S_m$ ) as (Fig.  
192 1):

$$193 S_m = S_{t\hat{n}} + Z_m, \quad (1)$$

194 where  $S_{t\hat{n}}$  is the spatial mean SWC at time  $t$  (temporal forcing) and  $Z_m$  is the  
195 spatial anomaly of SWC (lumped spatial forcing and interactions). The subscript  $\hat{n}$   
196 ( $\hat{t}$ ) indicates a space (time) averaged quantity.

197 According to Perry and Niemann (2007),  $S_{\hat{m}}$  can be estimated by remote sensing,  
198 water balance models, and in situ soil water measurement at a representative (or  
199 time-stable) location. The in situ soil water measurement method was selected  
200 because the representative location can be easily determined with prior SWC datasets.  
201 By measuring SWC only at the most time-stable location ( $s$ ) and future time  $t$  ( $S_{ts}$ ),  
202  $S_{\hat{m}}$  can be estimated using (Grayson and Western, 1998):

$$203 \quad S_{\hat{m}} = \frac{S_{ts}}{1 + \delta_{ts}} \quad , \quad (2)$$

204 where the  $s$  was identified using the time stability index of mean absolute bias error  
205 (Hu et al., 2010, 2012). The  $\delta_{ts}$  is the temporal mean relative difference of SWC at  
206 the  $s$ , which was calculated with prior measurements.

207 Spatial anomaly ( $Z_m$ ) can be reconstructed by the sum of the product of  
208 time-invariant spatial structures (EOFs) and temporally varying coefficients (ECs)  
209 using the EOF method (Perry and Niemann, 2007; Joshi and Mohanty, 2010;  
210 Vanderlinden et al., 2012). The ECs correspond to the eigenvectors of the matrix of  
211 spatial covariance of the  $Z_m$ , and the EOFs are obtained by projecting the  $Z_m$  onto  
212 the matrix ECs as: EOFs =  $Z_m$  ECs. The number of EOF (or EC) series equals the  
213 number of sampling dates. Each EOF series corresponds to one value at each location,  
214 and each EC series has one value at each measurement time. Each EOF is chosen to  
215 be orthogonal to other EOFs, and the lower-order EOFs account for as much variance  
216 as possible. The sum of variances of all EOFs equals the sum of variances of  $Z_m$   
217 from all measurement times.

218 Usually, a substantial amount of variance can be explained by a small number of

219 EOFs. Johnson and Wichern (2002) suggested the eigenvalue confidence limits  
 220 method for selecting the number of EOFs. Once the number of significant EOFs at a  
 221 confidence level of 95% is selected,  $Z_m$  can be estimated as the sum of the product  
 222 of significant EOFs and associated ECs as:

$$223 \quad Z_m = \sum \text{EOF}^{\text{sig}} \times (\text{EC}^{\text{sig}})^T, \quad (3)$$

224 where  $\text{EOF}^{\text{sig}}$  represents the significant EOFs of the  $Z_m$  obtained during model  
 225 development,  $\text{EC}^{\text{sig}}$  is the associated temporally varying coefficient, and the  
 226 superscript  $T$  represents matrix transpose. Following Perry and Niemann (2007), the  
 227 associated significant EC at time  $t$  ( $\text{EC}_t$ ), is estimated by the cosine relationship  
 228 between EC and  $S_{\hat{m}}$  developed using prior measurements:

$$229 \quad \text{EC}_t = a + b \cos\left(\frac{2\pi}{c} S_{\hat{m}} - d\right), \quad (4)$$

230 where  $a$ ,  $b$ ,  $c$ , and  $d$  are the fitted parameters using prior measurements and  $S_{\hat{m}}$  is  
 231 estimated from Eq. (2). By using the continuous function,  $\text{EC}_t$  can be estimated at  
 232 any  $S_{\hat{m}}$  values, which allows for the estimation of spatially distributed SWC at any  
 233 soil water conditions.

### 234 **2.2.2 The TA model**

235 Mittelbach and Seneviratne (2012) decomposed the  $S_m$  into a time-stable pattern  
 236 (i.e., temporal mean) and a temporal anomaly component (Fig. 1):

$$237 \quad S_m = M_{\hat{m}} + A_m, \quad (5)$$

238 where  $M_{\hat{m}}$  is the time-stable pattern (spatial forcing) controlled by “static” factors  
 239 such as soil properties and topography;  $A_m$  refers to the temporal anomaly (lumped  
 240 temporal forcing and interactions). The variance of SWC ( $\sigma_n^2(S_m)$ ) is the sum of

241 variance of the  $M_{\hat{m}}$  ( $\sigma_{\hat{m}}^2(M_{\hat{m}})$ ), variance of the  $A_{m}$  ( $\sigma_{\hat{m}}^2(A_m)$ ), and two times of  
 242 covariance between  $M_{\hat{m}}$  and  $A_m$  ( $2\text{cov}(M_{\hat{m}}, A_m)$ ), which can be expressed as:

$$243 \quad \sigma_{\hat{m}}^2(S_m) = \sigma_{\hat{m}}^2(M_{\hat{m}}) + 2\text{cov}(M_{\hat{m}}, A_m) + \sigma_{\hat{m}}^2(A_m). \quad (6)$$

244 Because the  $A_m$  in Mittelbach and Seneviratne (2012) is a lumped term, it can be  
 245 further decomposed into space-invariant temporal anomaly ( $A_{\hat{m}}$ , i.e., temporal  
 246 forcing) and space-variant temporal anomaly ( $R_m$ , i.e., interactions) (Vanderlinden et  
 247 al., 2012). At a watershed scale, the  $A_{\hat{m}}$  is controlled by temporally varying factors  
 248 such as meteorological variables and vegetation. Positive and negative  $A_{\hat{m}}$   
 249 correspond to relatively wet and dry periods, respectively. The  $R_m$  refers to the  
 250 redistribution of  $A_{\hat{m}}$  among different locations due to the interactions between  
 251 spatial forcing and temporal forcing. For example, soil and topography regulate how  
 252 much rainfall enters soil and how much water runs off or runs on at a location. This,  
 253 in turn, dictates vegetation growth in a water-limited environment. Therefore,  $S_m$   
 254 can also be expressed as (Fig. 1):

$$255 \quad S_m = M_{\hat{m}} + A_{\hat{m}} + R_m. \quad (7)$$

256 The temporal trends of  $A_{\hat{m}}$  in Eq. (7) and  $S_m$  in Eq. (1) are the same as both  
 257 represent temporal forcing. Because the  $A_{\hat{m}}$  is space-invariant and orthogonal to the  
 258  $M_{\hat{m}}$  and  $R_m$  in a space,  $\sigma_{\hat{m}}^2(S_m)$  in Eq. (6) can also be written as:

$$259 \quad \sigma_{\hat{m}}^2(S_m) = \sigma_{\hat{m}}^2(M_{\hat{m}}) + 2\text{cov}(M_{\hat{m}}, R_m) + \sigma_{\hat{m}}^2(R_m), \quad (8)$$

260 where  $\text{cov}(M_{\hat{m}}, R_m)$  is the covariance between the  $M_{\hat{m}}$  and  $R_m$ , and  $\sigma_{\hat{m}}^2(R_m)$  is  
 261 the variance of the  $R_m$ . Apparently,  $2\text{cov}(M_{\hat{m}}, R_m)$  equals  $2\text{cov}(M_{\hat{m}}, A_m)$ , and  
 262  $\sigma_{\hat{m}}^2(R_m)$  equals  $\sigma_{\hat{m}}^2(A_m)$ . The percent (%) ~~contributions~~ of  $\sigma_{\hat{m}}^2(M_{\hat{m}})$ ,

263  $2\text{cov}(M_{\hat{m}}, R_m)$ , and  $\sigma_{\hat{m}}^2(R_m)$  ~~to out of~~ the  $\sigma_{\hat{m}}^2(S_m)$  are calculated. The  
 264  $\text{cov}(M_{\hat{m}}, R_m)$  can be negative at some conditions, for example, when the depressions  
 265 correspond to greater  $M_{\hat{m}}$  and more negative  $R_m$  values in the discharge periods.  
 266 This resulted in percentage ~~contributions~~ of  $\sigma_{\hat{m}}^2(M_{\hat{m}})$  and  $\sigma_{\hat{m}}^2(R_m) > 100\%$  and  
 267 percentage ~~contributions~~ of  $2\text{cov}(M_{\hat{m}}, R_m) < 0\%$  (Mittelbach and Seneviratne, 2012;  
 268 Brocca et al., 2014; Rötzer et al., 2015). If  $R_m$  is zero at any time or location, there  
 269 are no interactions between spatial forcing and temporal forcing,  $\sigma_{\hat{m}}^2(S_m)$  and the  
 270 spatial trends of SWC are consistent over time. Therefore,  $R_m$  is directly  
 271 responsible for temporal change in the spatial variability of SWC.

272 If some underlying spatial patterns exist in  $R_m$ ,  $R_m$  can be reconstructed by the  
 273 sum of the product of time-invariant spatial structures (EOFs) and time-dependent  
 274 coefficients (ECs) using the EOF method. Note that the number of EOF (or EC) series  
 275 also equals the number of sampling dates.

276 For estimation of spatially distributed SWC,  $R_m$  is estimated by the same method  
 277 as  $Z_m$  using Eq. (3). The  $M_{\hat{m}}$  is estimated with prior measurements by:

$$278 \quad M_{\hat{m}} = \frac{1}{m} \sum_{j=1}^m S_m, \quad (9)$$

279 where  $m$  is the number of previous measurement times, and  $A_{\hat{m}}$   ~~$A_{\hat{m}}$~~  is estimated  
 280 by:

$$281 \quad A_{\hat{m}} = S_{\hat{m}} - M_{\hat{m}}, \quad (10)$$

282 where  $M_{\hat{m}}$  is the spatial mean of  $M_{\hat{m}}$ , and  $S_{\hat{m}}$  is estimated from SWC  
 283 measurements at the most time-stable location using Eq. (2).

284 The Pearson correlation coefficient ( $R$ ) is used to explore the linear relationships

Field Code Changed

285 between various spatial components in the two models (i.e., EOF1 of the  $Z_{tn}$  in the  
286 SA model,  $M_{\hat{tn}}$ , and EOF1 of the  $R_{tn}$  in the TA model) and environmental factors  
287 (i.e., soil, vegetative, and topographical properties). The multiple stepwise regressions  
288 are conducted to determine the percentage of variations in the spatial components  
289 which the controlling factors explain.

### 290 2.3 Validation and performance parameter

291 The TA model is more complicated than the SA model. In order to evaluate the two  
292 models for parsimony, AICc values are calculated (Burnham and Anderson, 2002) as:

$$293 \quad AICc = 2k + n \ln(RSS/n) + 2k(k+1)/(n-k-1), \quad (11)$$

294 where  $k$  is the number of parameters,  $n$  is the sample size, and  $RSS$  is the residual sum  
295 of squares.

296 Both cross validation and ~~external-split sample~~ validation are used to estimate SWC  
297 distribution with both models. For the cross validation, an iterative removal of 1 of the  
298 23 dates is made for model development, and the SWC along the transect  
299 corresponding to the removed date is estimated iteratively. For the ~~split~~  
300 ~~sample~~~~external~~ validation, SWC from 14 dates of the first two years (from July 17,  
301 2007 to May 27, 2009) is used for model development, and the SWC distribution of 9  
302 dates in the second two years (from July 21, 2009 to September 29, 2011) is  
303 estimated.

304 The Nash-Sutcliffe coefficient of efficiency (NSCE) is used to evaluate the quality  
305 of estimation of spatially distributed SWC, which is expressed as:

$$306 \quad NSCE = 1 - \frac{\sigma_{\epsilon}^2}{\sigma_{measure}^2}, \quad (12)$$

14



307 where  $\sigma_{measure}^2$  is the variance of measured SWC, and  $\sigma_{\varepsilon}^2$  is the mean squared  
308 estimation error. A larger NSCE value implies a better quality of estimation. A paired  
309 samples T-test is used to test whether the NSCE values between the TA model and the  
310 SA model are statistically significant at  $P < 0.05$ .

311 Many factors may affect the relative performance of spatially distributed SWC  
312 estimation between the TA model and the SA model. First, the degree of  
313 outperformance of the TA model over the SA model may depend on the amount of  
314  $R_{in}$  variance considered in the TA model. On one hand, the two models are identical  
315 if variance of  $R_{in}$  is close to zero or there are negligible interactions between the  
316 spatial and temporal components (Fig. 1). On the other hand, if no underlying spatial  
317 patterns exist in the  $R_{in}$  or the underlying spatial patterns ~~contributed~~ accounted for  
318 little ~~to the total~~ variance of the  $R_{in}$ , the outperformance will also be very limited.  
319 Therefore, the greater the variance of  $R_{in}$  considered in the TA model, the more  
320 likely the TA model can outperform the SA model. Second, the way of EOF  
321 decomposition may also affect the relative performance. In the SA model, EOF  
322 decomposition is performed on lumped time-stable patterns ( $M_{in}^{\wedge}$ ) and space-variant  
323 temporal anomaly ( $R_{in}$ ). In the TA model, however, EOF decomposition is made  
324 only on the  $R_{in}$ . In theory, the two models will be identical if the  $M_{in}^{\wedge}$  and the first  
325 underlying spatial pattern (i.e., EOF1) of the  $R_{in}$  were perfectly correlated. If a  
326 nonlinear relationship exists between them, lumping the  $M_{in}^{\wedge}$  and  $R_{in}$  together, as  
327 in the SA model, would weaken the model performance as compared to the TA model.  
328 From this aspect, the greater deviation from a linear relationship between the  $M_{in}^{\wedge}$

329 and EOF1 of the  $R_m$ , may lead to a greater outperformance of the TA model over  
330 the SA model. Finally, the performances of both models rely on the estimation  
331 accuracy of the  $EC_t$  which depends on both goodness of fit of the cosine function  
332 (i.e., Eq. 4) and estimation accuracy of the  $S_{in}$ . Because the same  $S_{in}$  values are  
333 used for the two models, the relative performance of the two models is related to the  
334 goodness of fit of Eq. (4).

### 335 **3. Results**

#### 336 **3.1 Components of SWC and their controls**

##### 337 **3.1.1 Spatial mean ( $S_{in}$ ) and spatial anomaly ( $Z_m$ )**

338 The values of spatial mean ( $S_{in}$ ) in the SA model varied with the seasons (Fig. 3a).  
339 In the spring, such as May 2, 2008 and April 20, 2009, snowmelt infiltration resulted  
340 in relatively great  $S_{in}$  values. In the summer, however, even one month after large  
341 rainfall events (such as on July 19, 2008 and June 21, 2009), the high  
342 evapotranspiration by fast-growing vegetation resulted in small  $S_{in}$  values. The  
343 values of  $S_{in}$  also varied between inter-annual meteorological conditions. In 2008,  
344 there was less precipitation and higher air temperature than in 2010 (Fig. 2). As a  
345 result,  $S_{in}$  was relatively smaller in 2008 than in 2010.

346 The spatial patterns of spatial anomaly ( $Z_m$ ) were similar to those of the original  
347 SWC patterns (Fig. 3a). The values of  $Z_m$  in wet periods (e.g., May 13, 2011) were  
348 much greater than in dry periods (e.g., August 23, 2008) in depressions (e.g., at a  
349 distance of 123 and 250 m); at other locations, however, the spatial anomaly was

350 slightly less in wet periods than in dry periods for both soil layers. Moreover, the  
351 spatial anomaly in depressions during the wet periods was much greater in the near  
352 surface than in the root zone.

353 When SWCs of all 23 dates were used for model development, only EOF1 was  
354 statistically significant (Fig. 4a), which accounted for 84.3% (0–0.2 m) and 86.5%  
355 (0–1.0 m) of the variances in the  $Z_m$ . Correlation analysis indicated that the spatial  
356 pattern of EOF1 in the  $Z_m$  was identical to the time-stable patterns ( $M_{\hat{m}}$ ) in the TA  
357 model ( $R=1.0$ ). The controls of EOF1 was therefore the same as those of  $M_{\hat{m}}$ , and  
358 will be discussed later. The relationship between associated EC1 and  $S_{\hat{m}}$  can be  
359 fitted well by the cosine function ( $R^2=0.73$  at both the near surface and root zone) (Fig.  
360 4b).

### 361 **3.1.2 Time-stable pattern ( $M_{\hat{m}}$ ), space-invariant temporal anomaly ( $A_{\hat{m}}$ ), and** 362 **space-variant temporal anomaly ( $R_m$ )**

363 Figure 3b displays the three components in the TA model. The first component  
364  $M_{\hat{m}}$  fluctuated along the transect, with high values in depressions and low values on  
365 knolls; the  $M_{\hat{m}}$  also had greater spatial variability in the near surface (variance  
366  $=36.7\%^2$ ) than in the root zone (variance $=19.5\%^2$ ). For both soil layers, SOC, depth to  
367 the  $\text{CaCO}_3$  layer, sand content, and wetness index are the dominant factors of  $M_{\hat{m}}$ ;  
368 they together explained 74.5% (near surface) and 75.6% (root zone) of the variances  
369 in the  $M_{\hat{m}}$  (Table 1). In addition, the temporal trend of  $A_{\hat{m}}$  was the same as that of  
370  $S_{\hat{m}}$  in the SA model (Fig. 3a) as both represent temporal forcing.

371 The  $R_m$  varied among landscape positions (Fig. 3b). At a sampling distance of

372 123 m (in a depression),  $R_m$  was negative in dry periods such as August 23, 2008 and  
 373 positive in wet periods such as May 13, 2011. This was true for all depressions for  
 374 both the near surface and the root zone. Therefore, topographically lower positions  
 375 usually corresponded to more positive  $R_m$  during the wet periods and more negative  
 376  $R_m$  during the dry periods. ~~This implies that topographically lower locations gained~~  
 377 ~~more water during recharge and lost more water during discharge due to the~~  
 378 ~~interactions of spatial and temporal forcing.~~ Furthermore, the absolute values of  $R_m$   
 379 were generally greater in the near surface than the root zone, indicating a greater  
 380 space-variant temporal anomaly for shallower depths.

381 The SWC variances and associated components (Eq. 8) also varied with time (Fig.  
 382 5). Often, wetter conditions corresponded to greater  $\sigma_{\hat{n}}^2(S_m)$ , as further indicated by  
 383 moderate correlation between  $\sigma_{\hat{n}}^2(S_m)$  and  $S_{\hat{n}}$  ( $R^2$  of 0.51 and 0.38 for the near  
 384 surface and the root zone, respectively). This was in agreement with others  
 385 (Gómez-Plaza et al., 2001; Martínez-Fernández and Ceballos, 2003; Hu et al., 2011).  
 386 Furthermore, there were greater  $\sigma_{\hat{n}}^2(S_m)$  values at near surface than in the root zone,  
 387 indicating greater variability of SWC in the near surface.

388 The time-invariant  $\sigma_{\hat{n}}^2(M_{\hat{n}})$  ~~contributed to~~ accounted for the  $\sigma_{\hat{n}}^2(S_m)$  with  
 389 percentages ranging from 25 to 795% for the near surface and from 40 to 174% for  
 390 the root zone (Fig. 5). The  $\sigma_{\hat{n}}^2(M_{\hat{n}})$  exceeded the  $\sigma_{\hat{n}}^2(S_m)$  mainly under dry  
 391 conditions, such as July–October in 2008 and 2009. This excess was offset by the  
 392  ~~$\sigma_{\hat{n}}^2(S_m)$~~   $\sigma_{\hat{n}}^2(R_m)$  and  $2 \text{cov}(M_{\hat{n}}, R_m)$ , with the latter ~~contributing~~ accounting for  
 393 ~~negatively to~~ the  $\sigma_{\hat{n}}^2(S_m)$  negatively with mean absolute percentages of 210% for

Field Code Changed

394 the near surface and 17% for the root zone. In the dry period, the ~~negative~~  
395 ~~contribution absolute percentage from of~~  $2\text{cov}(M_n, R_m)$  was up to 1327% for the  
396 near surface and 122% for the root zone. These values are comparable to those in  
397 Mittelbach and Seneviratne (2012) and Brocca et al. (2014).\_

398 The  $\sigma_n^2(R_m)$  ~~contributed~~ ~~accounted for less~~ ~~percentage of the~~  $\sigma_n^2(S_m)$  ~~than~~  
399 other components ~~did~~ (Fig. 5). The percentages of  $\sigma_n^2(R_m)$  ranged from 11 to 632%  
400 (arithmetic average of 118%) for the near surface and from 6 to 48% (arithmetic  
401 average of 19%) for the root zone; ~~the percentage of~~  $\sigma_n^2(R_m)$  tended to ~~contribute be~~  
402 ~~more greater~~ in drier periods. This indicates that the space-variant temporal anomaly  
403 cannot be ignored, particularly in dry conditions. Furthermore, the ~~contribution~~  
404 ~~percentage~~ of  $\sigma_n^2(R_m)$  was greater in the near surface than in the root zone,  
405 confirming stronger temporal dynamics of soil water at the near surface. Compared  
406 with larger scale studies (Mittelbach and Seneviratne, 2012; Brocca et al., 2014), ~~the~~  
407 ~~percentage of~~  $\sigma_n^2(R_m)$  ~~out of the~~  $\sigma_n^2(S_m)$  ~~of at~~ the near surface ~~contributed more to~~  
408  ~~$\sigma_n^2(S_m)$  was greater~~, with a mean percentage ~~contribution~~ of 118%, versus 9–68% in  
409 the other, larger scale studies. This indicates that interactions between spatial and  
410 temporal forcing were stronger, resulting in relatively more intensive temporal  
411 dynamics of soil water in our study area than at larger scales.

412 Three significant EOFs of  $R_m$  for both soil layers were identified when SWC of  
413 all 23 dates were used for model development. The first three EOFs explained 61.1,  
414 13.4, and 8.1% respectively, of the total  $R_m$  variance for the near surface, and 44.3,  
415 20.2, and 12.4%, respectively, of the total  $R_m$  variance in the root zone. Therefore,

Field Code Changed

Field Code Changed

416 our hypothesis that underlying spatial patterns exist in the  $R_m$  was  
417 ~~accepted~~supported. Due to the negligible contribution of EOF2 and EOF3 to the  
418 estimation of spatially distributed SWC, only EOF1 is shown in Fig. 6a. The  
419 associated EC1 changed with soil water conditions ( $S_m$ ) (Fig. 6b). When SWC was  
420 close to average levels, the EC1 was close to 0, resulting in negligible  $R_m$ . This was  
421 in accordance with Mittelbach and Seneviratne (2012) and Brocca et al. (2014), who  
422 showed that the spatial variance of the temporal anomaly was the smallest when water  
423 contents were close to average levels. The cosine function (Eq. 4) explained a large  
424 amount of the variances in EC1 for both soil layers ( $R^2=0.76$  at the near surface and  
425 0.88 in the root zone).

426 The contribution of EOF1 to the space-variant temporal anomaly can be examined  
427 through the product of the EOF1 and the associated EC1. The EC1 values tended to  
428 be positive during wet periods and negative during dry periods (Fig. 6b); more  
429 positive EOF1 values were usually observed at locations with greater  $M_m$  values  
430 (Figs. 3b and 6a). Therefore, the product of EOF1 and EC1 led to greater temporal  
431 SWC dynamics at wetter locations of both layers in both the wet and dry periods.

432 Depth to the  $\text{CaCO}_3$  layer and SOC had significant, positive correlations with  
433 EOF1 for both soil layers ( $R$  ranging from 0.76 to 0.88; Table 1). They jointly  
434 accounted for 81.6% (near surface) and 81.0% (root zone) of the variances in EOF1.  
435 This implies that locations with a greater depth to the  $\text{CaCO}_3$  layer and SOC, which  
436 correspond to wetter locations such as depressions, usually have greater temporal  
437 SWC dynamics during both wet and dry periods.

438 **3.2 Estimation of spatially distributed SWC**

439 When all 23 datasets were used and only EOF1 was considered, the TA model had  
440 an AICc value of 4093 for the near surface and 562 for the root zone, while the  
441 corresponding values for the SA model were 6370 and 3460. This indicated that even  
442 when penalty to complexity was given, the TA model was better than the SA model.  
443 The two models in terms of spatially distributed SWC estimation are compared below.

444 **3.2.1 The TA model**

445 The  $R_m$  terms and associated EOFs differed slightly with each validation. The  
446 number of significant EOFs varied between one (accounting for 60% of the total cases)  
447 and three for both soil layers. A paired samples T-test indicated that more EOFs did  
448 not result in a significant increase of NSCE in the estimation of spatially distributed  
449 SWC for both validation methods. ~~This is also supported by the increasing because~~  
450 AICc values ~~increased greatly~~ with the increasing number of parameters resulting  
451 from more EOFs (data not shown). This indicates that higher-order EOFs, even if they  
452 are statistically significant, are negligible for SWC prediction. Therefore, SWC  
453 distribution was estimated with EOF1 only.

454 Estimated SWCs generally approximated those measured at different soil water  
455 conditions during the cross validation (Fig. 7). However, on October 27, 2009, there  
456 were unsatisfactory overestimates at the 100–140 and 220–225 m locations near the  
457 surface (Fig. 7a). Unsatisfactory NSCE values of -4.05, -1.83, and -3.81 were  
458 obtained in the near surface in only three of the 23 dates, which were all in the fall  
459 (October 22, 2008, August 27, 2009, and October 27, 2009, respectively). The poor

460 performance obtained with the TA model on those dates (Fig. 8a) was a result of  
461 overestimation in depressions, which is shown for example on October 27, 2009 (Fig.  
462 7a), where strong evapotranspiration and deep drainage resulted in a much lower  
463 SWC than in the spring. These dates also corresponded to a high percentage of  
464 contribution of  $\sigma_n^2(R_m)$  to the  $\sigma_n^2(S_m)$  (203–439%). For August 23 and  
465 September 17 in 2008, which were in dry periods, the percentage of  $\sigma_n^2(R_m)$  of at  
466 the near surface was also contributed highly to the  $\sigma_n^2(S_m)$  (580 and 630%).  
467 Because a fair amount of  $\sigma_n^2(R_m)$  was accounted for with the TA model, the TA  
468 model performed satisfactorily (NSCE of 0.43 and 0.60). For the remaining 20 dates,  
469 the resulting NSCE value ranged from 0.38 to 0.90 in the near surface and from 0.65  
470 to 0.96 in the root zone (Fig. 8). This suggests that the TA model was generally  
471 satisfactory, with better performance in the root zone than in the near surface.

472 During the split sample external validation, the TA model resulted in SWC  
473 estimations with NSCE values ranging from 0.61 to 0.85 near the surface and from  
474 0.32 to 0.92 in the root zone, with exception of two days (August 27, 2009 and  
475 October 27, 2009 with NSCE values of -2.63 and -5.12, respectively) at 0–0.2 m (Fig.  
476 8). This suggested that the TA model performed well in estimating spatially  
477 distributed SWC patterns except on August 27, 2009 and October 27, 2009 at 0–0.2 m.  
478 The estimation in the root zone was also generally better than in the near surface.

### 479 3.2.2 Comparison with the SA model

480 One significant EOF of  $Z_m$  was identified for both soil layers, irrespective of the  
481 validation method. The SA model with only EOF1 produced reasonable SWC



482 estimations for both validations in all dates in the root zone and in every date except  
483 five dates (August 23, 2008, September 17, 2008, October 22, 2008, August 27, 2009,  
484 and October 27, 2009) in the near surface (Fig. 8). Similarly, when more EOFs were  
485 included, NSCE values did not increase significantly (data not shown) and  
486 consequently, estimation of spatially distributed SWC was not improved. This was  
487 because EOF2 and EOF3 together explained a very limited (<10%) amount of  
488 variability of  $Z_m$  and thus had low predictive power in terms of variance.

489 The difference in NSCE values between the TA and SA models for both validations  
490 are presented in Fig. 9. Generally, the difference decreased as  $A_{\hat{m}}$  increased, and  
491 then slightly increased with a further increase in  $A_{\hat{m}}$ . A paired samples T-test  
492 indicated that the NSCE values of the TA model were significantly ( $P<0.05$ ) greater  
493 than those of the SA model for both soil layers, irrespective of validation methods.  
494 This indicates that the TA model outperformed the SA model, particularly in dry  
495 conditions. This was because when the soil was dry, there was a high **contribution**  
496 **percentage** of  $\sigma_{\hat{n}}^2(R_m)$ , and thus strong variability in the space-variant temporal  
497 anomaly.

### 498 3.3 Further application at other two sites with different scales

#### 499 3.3.1 A hillslope in the Chinese Loess Plateau

500 ~~Along a hillslope of 100 m in length in the Chinese Loess Plateau, SWC of 0–0.06~~  
501 ~~m was measured 136 times from June 25, 2007 to August 30, 2008 by a Delta T~~  
502 ~~Devices Theta probe (ML2x) at 51 locations (Hu et al., 2011). The hillslope was~~  
503 ~~covered by *Stipa bungeana* Trin. and *Medicago sativa* L. in sandy loam and silt loam~~

504 ~~soils.~~ On average, the  $\sigma_{\hat{n}}^2(M_{in})$ ,  $\sigma_{\hat{n}}^2(R_m)$ , and  $2\text{cov}(M_{in}, R_m)$  ~~contributed~~  
505 ~~accounted for~~ 53, 74 and -27% ~~to-out of~~ the  $\sigma_{\hat{n}}^2(S_m)$ , indicating that both time-stable  
506 pattern and temporal anomalies were the main contributors to the  $\sigma_{\hat{n}}^2(S_m)$ . The EOF  
507 analysis showed that only the EOF1 was statistically significant for both the  $R_m$  and  
508  $Z_m$ , and the EOF1 explained 23% and 47% of the total variances of  $R_m$  and  $Z_m$ ,  
509 respectively. This illustrated that underlying spatial patterns exist in the  $R_m$  on the  
510 hillslope. Cross validation was used to estimate the spatially distributed SWC along  
511 the hillslope. The results showed that the NSCE varied from -4.25 to 0.83 (TA model)  
512 and from -4.30 to 0.81 (SA model), with a mean value of 0.25 and 0.19, respectively  
513 (Fig. 10a). A paired samples T-test showed that the NSCE values for the TA model  
514 were significantly ( $P < 0.05$ ) greater than those for the SA model, indicating that the  
515 TA model outperformed the SA model. As Fig. 10a shows, the outperformance was  
516 greater when SWC deviated from intermediate conditions, especially for dry  
517 conditions, which was similar to the Canadian site.

### 518 3.3.2 The GENCAI network in Italy

519 ~~In the GENCAI network (~250 km<sup>2</sup>) in Italy, SWC of 0–0.15 m was measured by a~~  
520 ~~TDR probe at 46 locations, 34 times from February to December in 2009 (Brocca et~~  
521 ~~al., 2012, 2013). The GENCAI area was dominated by grassland with a flat~~  
522 ~~topography, in silty clay soils.~~ The  $\sigma_{\hat{n}}^2(M_{in})$ ,  $\sigma_{\hat{n}}^2(R_m)$ , and  $2\text{cov}(M_{in}, R_m)$   
523 ~~contributed~~ ~~accounted for~~ 38, 68, and -7% ~~to-out of~~ the  $\sigma_{\hat{n}}^2(S_m)$  (Brocca et al.,  
524 2014), indicating the dominant ~~contribution role~~ of temporal anomalies ~~on-in~~ SWC  
525 variability. The first three EOFs of the  $R_m$  explained 19, 16, and 8% of the total

526  $\sigma_n^2(R_m)$ , and no EOFs were statistically significant, indicating that no underlying  
527 spatial patterns exist in the  $R_m$ . The EOF1 of the  $Z_m$  was significant and  
528 accounted for 37% of the variances in the  $Z_m$ . Although the EOF1 of the  $R_m$  was  
529 not significant, it was considered in the TA model for estimating spatially distributed  
530 SWC. The cross validation indicates that the NSCE varied from -0.79 to 0.50 (TA  
531 model) and from -0.87 to 0.56 (SA model), with mean values of 0.09 and 0.08,  
532 respectively (Fig. 10b). The SWC estimation based on these two models was not  
533 satisfactory except for a few days. As Fig. 10b shows, the differences in NSCE values  
534 between the two models were scattered around 0. A paired samples T-test showed that  
535 the NSCE values between the TA model and the SA model were not significant  
536 ( $P < 0.05$ ), indicating no differences in estimating spatially distributed SWC between  
537 these two models.

## 538 4 Discussion

### 539 4.1 Controls of the $M_{in}$ and $R_m$

540 The  $R_m$  played an important role in the temporal change in spatial patterns of the  
541 SWC. The underlying spatial patterns and physical meaning in the  $R_m$  were  
542 examined in our study for the first time. Although three significant EOFs of the  $R_m$   
543 existed in some cases, only EOF1 rather than higher-order EOFs of the  $R_m$  should  
544 be considered for the spatially distributed SWC estimation. Among many factors  
545 influencing the EOF1 of the  $R_m$ , depth to the  $\text{CaCO}_3$  layer followed by the SOC,  
546 were the most important factors. Depressions have deeper  $\text{CaCO}_3$  layers than knolls,

547 and the shallow CaCO<sub>3</sub> layer on knolls limited water infiltration during rainfall or  
548 snowmelt, resulting in less water recharge on knolls than in depressions. The depth to  
549 CaCO<sub>3</sub> layer and SOC were negatively correlated with elevation ( $R=-0.54$ ,  $P<0.01$ ).  
550 Therefore, the influence of depth to CaCO<sub>3</sub> layer and SOC partially reflected the role  
551 of topography in driving snowmelt runoff along slopes in the spring, which  
552 contributes to increasing water recharge in depressions. As already demonstrated,  
553 topographically lower positions corresponded to more negative  $R_m$  during the dry  
554 periods. This implies that depressions lost more water during discharge. This is  
555 because depressions ~~Locations with greater SOC~~ usually corresponded to vegetation  
556 with a larger leaf area index ( ~~$R=0.23$ ,  $P<0.05$~~ ), which would ~~also~~ result in higher  
557 evapotranspiration and more water loss during discharge periods.

558 As Table 1 shows, both the depth to the CaCO<sub>3</sub> layer and SOC controlled the  $M_{\hat{m}}$ .  
559 This was because deeper CaCO<sub>3</sub> layers and higher SOC were observed in depressions  
560 where soils were usually wetter in most of the year because of the snowmelt runoff in  
561 the spring and rainfall runoff in the summer and autumn (van der Kamp et al., 2003).  
562 Therefore, the roles of soil and topography were two-fold: On one hand, they were  
563 highly correlated with the time-stable patterns and thus the time stability of SWC  
564 (Gómez-Plaza et al., 2000; Mohanty and Skaggs, 2001; Grant et al., 2004); On the  
565 other hand, soil and topography, interplaying with temporal forcing, triggered  
566 local-specific soil water change and destroyed time stability of SWC. Their roles in  
567 protecting time stability persisted, but their roles in destroying time stability varied  
568 with time. Greater  $\sigma_n^2(R_m)$  implies greater contribution of these factors in soil water

Field Code Changed

569 dynamics, resulting in less time stability of SWC.

#### 570 4.2 Model performance for spatially distributed SWC estimation

571 The outperformance of the TA model for estimating spatial SWC at the Canadian  
572 site and Chinese site can be partly explained by the high ~~contribution~~ percentages  
573 (average of 19–118%) of the  $\sigma_n^2(R_m)$  ~~to out of~~ the total variance. When SWC is  
574 close to average levels,  $R_m$  is also close to zero, resulting in negligible ~~variance~~  
575 ~~contribution percentage from of~~  $\sigma_n^2(R_m)$   ~~$R_m$  to the total variance~~. In this case, the  
576 soil water patterns are stable in time, the SA model performs well, and there will be  
577 little differences between these two models. As is well known, the spatial patterns in  
578 soil water content are inherently time unstable. For example, when evapotranspiration  
579 becomes the dominant process at the small watershed scale, more water will be lost in  
580 depressions due to the denser vegetation than on knolls (Millar, 1971; Biswas et al.,  
581 2012), effectively diminishing the spatial patterns and increasing temporal instability.  
582 In this case, the  $\sigma_n^2(R_m)$  ~~contributes~~ accounts for more ~~to percentage of~~ the total  
583 variance (e.g., high up to 632%) and the TA model may outperform the SA model.  
584 This explained why the outperformance of the TA model was more obvious in the dry  
585 conditions. For the GENCAI network in Italy, although the  $\sigma_n^2(R_m)$  ~~contributed~~  
586 accounted for 68% of the total variance, the performance of the TA model was  
587 identical to the SA model. This was because there were no underlying spatial patterns  
588 in the  $R_m$ . Similarly, because the first underlying spatial pattern (i.e., EOF1)  
589 explained greater percentages of the  $\sigma_n^2(R_m)$  at the Canadian site (44–61%) than the  
590 Chinese site (23%), the outperformance of the TA model over the SA model was more

Field Code Changed

591 obvious at the former site (Fig. 9 and 10a). Therefore, the TA model is advantageous  
592 only if the ~~contribution percentage~~ of  $\sigma_n^2(R_m)$  ~~to-out of~~ the total variance is  
593 substantial and underlying spatial patterns exist in the  $R_m$ .

594 The existence of underlying spatial patterns in the  $R_m$  is related to the controlling  
595 factors, which may be scale-specific. At small scales, “static” factors such as the depth  
596 to the  $\text{CaCO}_3$  layer and SOC at the Canadian site may affect not only the time-stable  
597 patterns but also the  $R_m$ . The persistent influence of “static” factors on the  $R_m$   
598 resulted in significant underlying spatial patterns in the  $R_m$ . Thus, the TA model  
599 outperformed the SA model at the small scales. At large scales such as the basin scale  
600 or greater, time-stable patterns may be controlled by, in addition to soil and  
601 topography (Mittelbach and Seneviratne, 2012), the climate gradient (Sherratt and  
602 Wheeler, 1984); at those scales,  $R_m$  is more likely to be controlled by the  
603 meteorological anomaly (i.e., spatially random variation) (Walsh and Mostek, 1980),  
604 and the effects of soil and topography may be reduced. Consequently, spatial patterns  
605 in the  $R_m$  may be weakened and the TA model may have no advantages over the SA  
606 model such as for the Italian site.

607 The  $M_{\hat{m}}$  and the underlying spatial patterns (EOF1) in the  $R_m$  were controlled  
608 by the same spatial forcing (e.g., depth to  $\text{CaCO}_3$  layer and SOC) at the Canadian site  
609 (Table 1), and they were correlated with an  $R^2$  of 0.83 for the near surface and 0.42 for  
610 the root zone. Although the relationships between  $M_{\hat{m}}$  and  $R_m$  were strong, they  
611 were not strictly linear, suggesting that  $M_{\hat{m}}$  and  $R_m$  were affected differently by  
612 these factors. Therefore, the nonlinear relationship between  $M_{\hat{m}}$  and  $R_m$  partially

613 contributed to the outperformance of the TA model over the SA model.

614 The relationship between the  $S_{\hat{m}}$  and EC1 was better fitted by the cosine function  
615 in the TA model than the SA model (Figs. 4b and 6b), with  $R^2$  of 0.76 versus 0.73 in  
616 the near surface and 0.88 versus 0.73 in the root zone. The reduced scatter in the  $S_{\hat{m}}$   
617 and EC1 relationship for the TA model may also partly explain the outperformance of  
618 the TA model over the SA model.

619 Therefore, the outperformance of the TA model over the SA model depends on  
620 counterbalance among the variance of  $R_{m}$  explained in the TA model, the linear  
621 correlation between the  $M_{\hat{m}}$  and EOF1 of the  $R_{m}$ , and the goodness of fit for the  
622  $S_{\hat{m}}$  and EC1 relationship. For example, the variance of EOF1 in the  $R_{m}$  for the  
623 near surface (i.e., 264%<sup>2</sup>) was much greater than that for the root zone (i.e., 43%<sup>2</sup>).  
624 However,  $M_{\hat{m}}$  and underlying spatial patterns (EOF1) in the  $R_{m}$  in the root zone  
625 deviated more from a linear relationship, and the reduced scatter in the  $S_{\hat{m}}$  and EC1  
626 relationship in the TA model was more obviously in the root zone than in the near  
627 surface. As a result, the outperformance of the TA model was comparable between the  
628 near surface and root zone at the Canadian site (Fig. 9).

629 In the real world, the relations between the  $M_{\hat{m}}$  and underlying spatial patterns in  
630 the  $R_{m}$  may rarely be perfectly linear. Therefore, when underlying spatial patterns  
631 exist in the  $R_{m}$  and the  $R_{m}$  has substantial variances, the TA model is preferable  
632 to the SA model for the estimation of spatially distributed SWC. On the contrary,  
633 when underlying spatial patterns does not exist in the  $R_{m}$  or the  $R_{m}$  has negligible  
634 variances, the SA model may be selected although these two models yield the same

Field Code Changed

Field Code Changed

635 ~~quality of SWC estimation. This is because Because the TA model was not worse than~~  
636 ~~the SA model for the whole range of SWC, the TA model is suggested for the~~  
637 ~~estimation of spatially distributed SWC at different soil water conditions. the TA~~  
638 ~~model needs one more spatial parameter (i.e.,  $M_{in}$ ) than the SA model.~~

639 Previous studies on SWC decomposition mainly focus on near surface layers  
640 (Jawson and Niemann, 2007; Perry and Niemann, 2007, 2008; Joshi and Mohanty,  
641 2010; Korres et al., 2010; Busch et al., 2012). This study decomposed spatiotemporal  
642 SWC using the TA model for both the near surface and the root zone. The results  
643 showed that the estimation of spatially distributed SWC at small watershed scales was

644 improved by the TA method that considers the  $R_m$ . ~~The  $\sigma_n^2(M_{in})$  was greater than~~  
645 ~~the  $\sigma_n^2(R_m)$  (Fig. 5), indicating that time stability was more important than time~~  
646 ~~instability for SWC estimation. For the three dates in the fall (i.e., October 22, 2008,~~  
647 ~~August 27, 2009, and October 27, 2009), strong evapotranspiration and deep drainage~~  
648 ~~in depressions resulted in a much lower SWC at the near surface than in the spring.~~  
649 ~~This resulted in reduced time stability of SWC pattern and poor performance of both~~  
650 ~~models and validation methods in terms of SWC evaluation (Fig. 8a).~~ Because of the

651 stronger time stability of SWC in deeper soil layers (Biswas and Si, 2011), SWC  
652 evaluation ~~was more accurate in for thicker soil layers extending from the surface to~~  
653 ~~greater depth was more accurate than in shallow soil layers.~~ This is particularly  
654 important because SWC data for deeper soil layers in a watershed is more difficult to  
655 collect than that of surface soil.

Field Code Changed

Field Code Changed

Field Code Changed



## 656 5 Conclusions

657 The TA model was used to decompose spatiotemporal SWC into time-stable  
658 patterns  $M_{in}^{\wedge}$ , space-invariant temporal anomaly  $A_{in}^{\wedge}$ , and space-variant temporal  
659 anomaly  $R_{in}$ . This study indicated that underlying spatial patterns may exist in the  
660  $R_{in}$  at small scales (e.g., small watersheds and hillslope) but may not exist at large  
661 scales such as the GENCAI network (~250 km<sup>2</sup>) in Italy. This was because the  $R_{in}$   
662 at small scales was driven by “static” factors such as depth to the CaCO<sub>3</sub> layer and  
663 SOC at the Canadian site, while the  $R_{in}$  at large scales may be dominated by  
664 “dynamic” factors such as meteorological anomaly. Compared to the SA model,  
665 estimation of spatially distributed SWC was improved with the TA model at small  
666 watershed scales. This was because the TA model considered a fair amount of spatial  
667 variance in the  $R_{in}$ , which was ignored in the SA model. Furthermore, the improved  
668 performance was observed mainly when there was less or more soil water than the  
669 average level, especially in drier conditions due to the high  $\sigma_n^2(R_m)$  value.

670 This study showed that outperformance of the TA model over the SA model is  
671 possible when  $\sigma_n^2(R_m)$  ~~contributes~~ accounts for substantial ~~variance to the total~~  
672 variance of SWC, and significant spatial patterns (or EOFs) exist in the  $R_{in}$ . Further  
673 application of the TA model for the estimation of spatially distributed SWC at  
674 different scales and hydrological backgrounds is recommended. If the TA model  
675 parameters (i.e.,  $M_{in}^{\wedge}$ , EOF1 of the  $R_{in}$ , and relationship between EC and  $S_{in}$ ) are  
676 obtained from historical in-situ SWC datasets, a detailed spatially distributed SWC of  
677 near surface soil at watershed scales can be constructed from remotely sensed SWC.

678 Note that both models rely on ~~previous~~ in-situ SWC measurements for model  
679 parameters. Therefore, ~~the future study-research~~ should be ~~directed-conducted~~ to  
680 estimate spatially distributed SWC in un-gauged watersheds based on the estimation  
681 of the model parameters using pedotransfer functions. ~~Since the TA model needs one~~  
682 ~~more spatial parameter (i.e.,  $M_{in}$ ) than the SA model, the advantage of the TA model~~  
683 ~~may be weakened. Nevertheless, the TA model may be preferred if it estimates spatial~~  
684 ~~SWC much better than the SA model such as under dry conditions.~~ The codes for  
685 decomposing SWC with the SA and TA models and related EOF analysis were written  
686 in Matlab and are freely available from the authors upon request.

## 687 **Acknowledgements**

688 This project was funded by [the National Science Foundation of China \(K305021308\)](#)  
689 ~~and~~ the Natural Sciences and Engineering Research Council (NSERC) of Canada. We  
690 thank Dr. Asim Biswas, Dr. Henry Wai Chau, Mr. Trent Pernitsky, and Mr. Eric Neil  
691 for their help in data collection. We thank the anonymous reviewers and the Editor for  
692 their constructive comments.

## 693 **References**

694 Biswas, A., Chau, H. W., Bedard-Haughn, A., and Si, B. C.: Factors controlling soil  
695 water storage in the Hummocky landscape of the Prairie Pothole region of North  
696 America, Can. J. Soil Sci., 92, 649–663, doi: 10.4141/CJSS2011-045, 2012.  
697 Biswas, A. and Si, B. C.: Scales and locations of time stability of soil water storage in

698 a hummocky landscape, *J. Hydrol.*, 408, 100–112, doi: 10.1016/j.jhydrol.2011.07.027,  
699 2011.

700 Blöschl, G., Komma, J., and Hasenauer, S.: Hydrological downscaling of soil  
701 moisture, Final report to the H-SAF (Hydrology Satellite Application Facility) via the  
702 Austrian Central Institute for Meteorology and Geodynamics (ZAMG), Vienna  
703 University of Technology, A-1040 Vienna, Austria, 2009.

704 Brocca, L., Melone, F., Moramarco, T., and Morbidelli, R.: Soil moisture temporal  
705 stability over experimental areas in Central Italy, *Geoderma*, 148, 364–374, doi:  
706 10.1016/j.geoderma.2008.11.004, 2009.

707 Brocca, L., Tullo, T., Melone, F., Moramarco, T., and Morbidelli, R.: Catchment scale  
708 soil moisture spatial-temporal variability, *J. Hydrol.*, 422-423, 63–75,  
709 doi:10.1016/j.jhydrol.2011.12.039, 2012.

710 Brocca, L., Zucco, G., Mittelbach, H., Moramarco, T., and Seneviratne, S. I.: Absolute  
711 versus temporal anomaly and percent of saturation soil moisture spatial variability for  
712 six networks worldwide, *Water Resour. Res.*, 50, 5560–5576, doi:  
713 10.1002/2014WR015684, 2014.

714 Brocca, L., Zucco, G., Moramarco, T., and Morbidelli, R.: Developing and testing a  
715 long-term soil moisture dataset at the catchment scale, *J. Hydrol.*, 490, 144–151, doi:  
716 10.1016/j.jhydrol.2013.03.029, 2013.

717 Burnham, K. P. and Anderson, D. R.: Model selection and multimodel inference: A  
718 practical information-theoretic approach (2nd ed.), Springer-Verlag, New York, 2002.

719 Busch, F. A., Niemann, J. D., and Coleman, M.: Evaluation of an empirical

720 orthogonal function-based method to downscale soil moisture patterns based on  
721 topographical attributes, *Hydrol. Process.*, 26, 2696–2709, doi: 10.1002/hyp.8363,  
722 2012.

723 Champagne, C., Berg, A. A., McNairn, H., Drewitt, G., and Huffman, T.: Evaluation  
724 of soil moisture extremes for agricultural productivity in the Canadian prairies, *Agric.  
725 For. Meteorol.*, 165, 1–11, doi: 10.1016/j.agrformet.2012.06.003, 2012.

726 Famiglietti, J. S., Rudnicki, J. W., and Rodell, M.: Variability in surface moisture  
727 content along a hillslope transect: Rattlesnake Hill, Texas, *J. Hydrol.*, 210, 259–281,  
728 doi: 10.1016/S0022-1694(98)00187-5, 1998.

729 Gómez-Plaza, A., Alvarez-Rogel, J., Albaladejo, J., and Castillo, V. M.: Spatial  
730 patterns and temporal stability of soil moisture across a range of scales in a semi-arid  
731 environment, *Hydrol. Process.*, 14, 1261–1277, doi:  
732 10.1002/(SICI)1099-1085(200005)14:7<1261::AID-HYP40>3.0.CO;2-D, 2000.

733 Gómez-Plaza, A., Martínez-Mena, M., Albaladejo, J., and Castillo, V. M.: Factors  
734 regulating spatial distribution of soil water content in small semiarid catchments, *J.  
735 Hydrol.*, 253, 211–226, doi: 10.1016/S0022-1694(01)00483-8, 2001.

736 Grant, L., Seyfried, M., and McNamara, J.: Spatial variation and temporal stability of  
737 soil water in a snow-dominated, mountain catchment, *Hydrol. Process.*, 18,  
738 3493–3511, doi: 10.1002/hyp.5789, 2004.

739 Grayson, R. B. and Western, A. W.: Towards areal estimation of soil water content  
740 from point measurements: Time and space stability of mean response, *J. Hydrol.*, 207,  
741 68–82, doi: 10.1016/S0022-1694(98)00096-1, 1998.

742 Hu, W., Shao, M. A., Han, F. P., and Reichardt, K.: Spatio-temporal variability  
743 behavior of land surface soil water content in shrub- and grass-land, *Geoderma*, 162,  
744 260–272, doi: 10.1016/j.geoderma.2011.02.008, 2011.

745 Hu, W., Shao, M. A., and Reichardt, K.: Using a new criterion to identify sites for  
746 mean soil water storage evaluation, *Soil Sci. Soc. Am. J.*, 74, 762–773, doi:  
747 10.2136/sssaj2009.0235, 2010.

748 Hu, W., Tallon, L. K., and Si, B. C.: Evaluation of time stability indices for soil water  
749 storage upscaling, *J. Hydrol.*, 475, 229–241, doi: 10.1016/j.jhydrol.2012.09.050,  
750 2012.

751 Jawson, S. D. and Niemann, J. D.: Spatial patterns from EOF analysis of soil moisture  
752 at a large scale and their dependence on soil, land-use, and topographic properties,  
753 *Adv. Water Resour.*, 30, 366–381, doi:10.1016/j.advwatres.2006.05.006, 2007.

754 Jia, Y. H. and Shao, M. A.: Temporal stability of soil water storage under four types of  
755 revegetation on the northern Loess Plateau of China, *Agric. Water Manage.*, 117,  
756 33–42, doi: 10.1016/j.agwat.2012.10.013, 2013.

757 Johnson, R. A. and Wichern, D. W.: *Applied multivariate statistical analysis*, Prentice  
758 Hall, Upper Saddle River, New Jersey, 2002.

759 Joshi, C. and Mohanty, B. P.: Physical controls of near-surface soil moisture across  
760 varying spatial scales in an agricultural landscape during SMEX02, *Water Resour.*  
761 *Res.*, 46, doi: 10.1029/2010WR009152, 2010.

762 Korres, W., Koyama, C. N., Fiener, P., and Schneider, K.: Analysis of surface soil  
763 moisture patterns in agricultural landscapes using Empirical Orthogonal Functions,

764 Hydrol. Earth Syst. Sci., 14, 751–764, doi: 10.5194/hess-14-751-2010, 2010.

765 Martínez-Fernández, J. and Ceballos, A.: Temporal stability of soil moisture in a  
766 large-field experiment in Spain, *Soil Sci. Soc. Am. J.*, 67, 1647–1656, 2003.

767 Millar, J. B.: Shoreline-area ratios as a factor in rate of water loss from small sloughs,  
768 *J. Hydrol.*, 14, 259–284, doi: 10.1016/0022-1694(71)90038-2, 1971.

769 Mittelbach, H. and Seneviratne, I.: A new perspective on the spatio-temporal  
770 variability of soil moisture: Temporal dynamics versus time-invariant contributions,  
771 *Hydrol. Earth Syst. Sci.*, 16, 2169–2179, doi: 10.5194/hess-16-2169-2012, 2012.

772 Mohanty, B. P. and Skaggs, T. H.: Spatio-temporal evolution and time-stable  
773 characteristics of soil moisture within remote sensing footprints with varying soil  
774 slope and vegetation, *Adv. Water Resour.*, 24, 1051–1067, doi:  
775 10.1016/S0309-1708(01)00034-3, 2001.

776 Peel, M. C., Finlayson, B. L., and McMahon, T. A.: Updated world map of the  
777 Köppen-Geiger climate classification, *Hydrol. Earth Syst. Sci.*, 11, 1633–1644,  
778 doi:10.5194/hess-11-1633-2007, 2007.

779 Perry, M. A. and Niemann J. D.: Analysis and estimation of soil moisture at the  
780 catchment scale using EOFs, *J. Hydrol.*, 334, 388–404, doi:  
781 10.1016/j.jhydrol.2006.10.014, 2007.

782 Perry, M. A. and Niemann J. D.: Generation of soil moisture patterns at the catchment  
783 scale by EOF interpolation, *Hydrol. Earth Syst. Sci.*, 12, 39–53,  
784 doi:10.5194/hess-12-39-2008, 2008.

785 Robinson, D. A., Campbell, C. S., Hopmans, J. W., Hornbuckle, B. K., Jones, S. B.,

786 Knight, R., Ogden, F., Selker, J., and Wendroth, O.: Soil moisture measurement for  
787 ecological and hydrological watershed-scale observatories: A review, *Vadose Zone J.*,  
788 7, 358–389, doi: 10.2136/vzj2007.0143, 2008.

789 Rötzer, K., Montzka, C., and Vereecken, H.: Spatio-temporal variability of global soil  
790 moisture products, *J. Hydrol.*, 522, 187–202, doi: 10.1016/j.jhydrol.2014.12.038,  
791 2015.

792 She, D. L., Liu, D. D., Peng, S. Z., and Shao, M. A.: Multiscale influences of soil  
793 properties on soil water content distribution in a watershed on the Chinese Loess  
794 Plateau, *Soil Sci.*, 178, 530–539, doi: 10.1016/j.jhydrol.2014.08.034, 2013a.

795 She, D. L., Xia, Y. Q., Shao, M. A., Peng, S. Z., and Yu, S. E.: Transpiration and  
796 canopy conductance of *Caragana Korshinskii* trees in response to soil moisture in  
797 sand land of China, *Agrofor. Syst.*, 87, 667–678, doi: 10.1007/s10457-012-9587-4,  
798 2013b.

799 Sherratt, D. J. and Wheeler, H. S.: The use of surface-resistance soil-moisture  
800 relationships in soil-water budget models, *Agric. For. Meteorol.*, 31, 143–157, doi:  
801 10.1016/0168-1923(84)90016-9, 1984.

802 Soil Survey Staff: *Soil Taxonomy*, 11th edition, USDA National Resources  
803 Conservation Services, Washington DC, 2010.

804 Starr, G. C.: Assessing temporal stability and spatial variability of soil water patterns  
805 with implications for precision water management, *Agric. Water Manage.*, 72,  
806 223–243, doi: 10.1016/j.agwat.2004.09.020, 2005.

807 Vachaud, G., De Silans, A. P., Balabanis, P., and Vauclin, M.: Temporal stability of

808 spatially measured soil water probability density function, *Soil Sci. Soc. Am. J.*, 49,  
809 822–828, 1985.

810 van der Kamp, G., Hayashi, M., and Gallen, D.: Comparing the hydrology of grassed  
811 and cultivated catchments in the semi-arid Canadian prairies, *Hydrol. Process.*, 17,  
812 559–575, doi: 10.1002/hyp.1157, 2003.

813 Vanderlinden, K., Vereecken, H., Hardelauf, H., Herbst, M., Martinez, G., Cosh, M.  
814 H., and Pachepsky, Y. A.: Temporal stability of soil water contents: A review of data  
815 and analyses, *Vadose Zone J.*, 11, 4, doi: 10.2136/vzj2011.0178, 2012.

816 Vereecken, H., Kamai, T., Harter, T., Kasteel, R., Hopmans, J., and Vanderborght, J.:  
817 Explaining soil moisture variability as a function of mean soil moisture: A stochastic  
818 unsaturated flow perspective, *Geophys. Res. Lett.*, 34, L22402, doi:  
819 10.1029/2007GL031813, 2007.

820 Venkatesh, B., Nandagiri, L., Purandara, B. K., and Reddy, V. B.: Modelling soil  
821 moisture under different land covers in a sub-humid environment of Western Ghats,  
822 India, *J. Earth Syst. Sci.*, 120, 387–398, 2011.

823 Walsh, J. E. and Mostek, A.: A quantitative-analysis of meteorological anomaly  
824 patterns over the United-States, 1900–1977, *Mon. Weather Rev.*, 108, 615–630, doi:  
825 10.1175/1520-0493(1980)108<0615:AQAOMA>2.0.CO;2, 1980.

826 Wang, Y. Q., Shao, M. A., Liu, Z. P., and Warrington, D. N.: Regional spatial pattern  
827 of deep soil water content and its influencing factors, *Hydrolog. Sci. J.*, 57, 265–281,  
828 doi: 10.1080/02626667.2011.644243, 2012.

829 Ward, P. R., Flower, K. C., Cordingley, N., Weeks, C., and Micin, S. F.: Soil water



830 balance with cover crops and conservation agriculture in a Mediterranean climate,  
831 *Field Crop. Res.*, 132, 33–39, doi: 10.1016/j.fcr.2011.10.017, 2012.

832 Zhao, Y., Peth, S., Wang, X. Y., Lin, H., and Horn, R.: Controls of surface soil  
833 moisture spatial patterns and their temporal stability in a semi-arid steppe, *Hydrol.*  
834 *Process.*, 24, 2507–2519, doi: 10.1002/hyp.7665, 2010.

835 **Figure captions**

836 **Figure 1.** Decomposition of spatiotemporal soil water content (SWC) in different  
837 models.

838 **Figure 2.** Daily mean air temperature and precipitation during the study period.

839 **Figure 3.** Components of soil water content in (a) the SA model (spatial mean soil  
840 water content  $S_{\hat{m}}$  and spatial anomaly  $Z_m$ ) and in (b) the TA model (time-stable  
841 pattern  $M_{\hat{m}}$ , space-invariant temporal anomaly  $A_{\hat{m}}$ , and space-variant temporal  
842 anomaly  $R_m$ ) for 0–0.2 and 0–1.0 m. Also shown is the elevation.

843 **Figure 4.** (a) The EOF1 of the spatial anomaly  $Z_m$  and (b) relationships of  
844 associated EC1 versus spatial mean soil water content  $Z_m$  fitted by the cosine  
845 function (Eq. 4).

846 **Figure 5.** Spatial variances of different components in Eq. (8) expressed in %<sup>2</sup> (upper  
847 panel) and as percentage (lower panel) for (a) 0–0.2 and (b) 0–1.0 m. Spatial mean  
848 soil water content  $S_{\hat{m}}$  on each measurement day is also shown.

849 **Figure 6.** (a) The EOF1 of the space-variant temporal anomaly  $R_m$  and (b)  
850 relationships of associated EC1 versus spatial mean soil water content  $S_{\hat{m}}$  fitted by  
851 the cosine function (Eq. 4).

852 **Figure 7.** Estimated soil water content (SWC) versus measured SWC for three dates  
853 at different soil water conditions (August 23, 2008, October 27, 2009, and May 13,  
854 2011 are associated with relatively dry, medium, and wet days, respectively) using the  
855 TA model for (a) 0–0.2 and (b) 0–1.0 m.

856 **Figure 8.** The Nash-Sutcliffe coefficient of efficiency (NSCE) of soil water content

857 estimation using the TA and SA models for (a) 0–0.2 and (b) 0–1.0 m for both cross  
858 validation (CV) and ~~split sample~~external validation (EVS<sub>V</sub>). At 0–0.2 m, three dates  
859 (October 22, 2008, August 27, 2009, and October 27, 2009) as indicated by green  
860 lines present negative NSCE values (-4.05, -1.83, and -3.81, respectively, for the CV  
861 on the three dates; -2.63 and -5.12, respectively, for the SV on the latter two  
862 dates).~~negative Nash-Sutcliffe coefficient of efficiency values for three dates (October~~  
863 ~~22, 2008, August 27, 2009, and October 27, 2009) are not shown.~~ Spatial mean soil  
864 water content  $S_{in}$  on each measurement day is also shown.

865 **Figure 9.** ~~Difference between the~~Nash-Sutcliffe coefficient of efficiency (NSCE)  
866 difference between the TA and SA models in terms of soil water content estimation  
867 by using both cross validation (CV) and ~~split sample~~external validation (EVS<sub>V</sub>) using  
868 ~~the TA and SA models~~ as a function of space-invariant temporal anomaly  $A_{in}$  for (a)  
869 0–0.2 and (b) 0–1.0 m.

870 **Figure 10.** ~~Difference between the~~Nash-Sutcliffe coefficient of efficiency (NSCE)  
871 difference between the TA and SA models in terms of soil water content estimation  
872 using cross validation of soil water content evaluation by the cross validation using  
873 ~~the TA and SA models~~ as a function of space-invariant temporal anomaly  $A_{in}$  for (a)  
874 0–0.06 m of the Chinese Loess Plateau hillslope and (b) 0–0.15 m of the GENCAI  
875 network in Italy. The NSCE values for both models are also shown.

**Table 1.** Pearson correlation coefficients between time-stable pattern  $M_{\hat{m}}$ , EOF1 of space-variant temporal anomaly  $R_{tm}$  and various properties.

	0–0.2 m		0–1.0 m	
	$M_{\hat{m}}$	EOF1	$M_{\hat{m}}$	EOF1
Sand content	-0.52**	-0.36**	-0.66**	-0.26**
Silt content	0.29**	0.14	0.40**	0.06
Clay content	0.43**	0.38**	0.51**	0.33**
Organic carbon	0.78**	0.83**	0.73**	0.76**
Wetness index	0.64**	0.59**	0.68**	0.56**
Depth to CaCO <sub>3</sub> layer	0.77**	0.84**	0.65**	0.88**
A horizon depth	0.51**	0.62**	0.44**	0.65**
C horizon depth	0.66**	0.69**	0.58**	0.76**
Bulk density	-0.58**	-0.67**	-0.46**	-0.62**
Elevation	-0.24**	-0.28**	-0.24**	-0.32**
Specific contributing area	0.20*	0.24**	0.24**	0.23**
Convergence index	-0.58**	-0.56**	-0.55**	-0.58**
Curvature	-0.10	-0.08	-0.19*	-0.16
Cos(aspect)	0.05	0.04	0.08	0.05
Gradient	-0.12	-0.09	-0.21*	-0.02
Slope	-0.51**	-0.48**	-0.56**	-0.44**
Upslope length	0.19*	0.21*	0.21*	0.25**
Solar radiation	-0.07	0.03	-0.11	0.08
Flow connectivity	0.45**	0.43**	0.49**	0.49**
Leaf area index	-0.07	0.06	-0.10	-0.14
Variance explained <sup>1</sup>	74.5%	81.6%	75.6%	81.0%

<sup>1</sup>percent of variance explained by the controlling factors obtained by the multiple stepwise regressions.

\*Significant at  $P < 0.05$ ; \*\* Significant at  $P < 0.01$ .

**Table A1.** Notations.

---

$M_{\hat{n}}$	spatial mean of $M_{\hat{n}}$
$R_{tn}$	space-variant temporal anomaly of SWC at location $n$ and time $t$
$A_{\hat{n}}$	space-invariant temporal anomaly of SWC at time $t$
$Z_{tn}$	spatial anomaly of SWC at location $n$ and time $t$
$S_{\hat{n}}$	spatial mean SWC at time $t$
$\sigma_{\hat{n}}^2$	spatial variance
$A_{tn}$	temporal anomaly of SWC at location $n$ and time $t$
$\delta_{\hat{n}}$	temporal mean relative difference of SWC at location $n$
COV	spatial covariance
$S_{tn}$	SWC at location $n$ and time $t$
$M_{\hat{n}}$	time-stable pattern of SWC
ECs	temporally-varying coefficients of $R_{tn}$ (or $Z_{tn}$ )
EOFs	time-invariant spatial structures of $R_{tn}$ (or $Z_{tn}$ )
NSCE	Nash-Sutcliffe coefficient of efficiency
$R$	Pearson correlation coefficient
SWC	soil water content

---

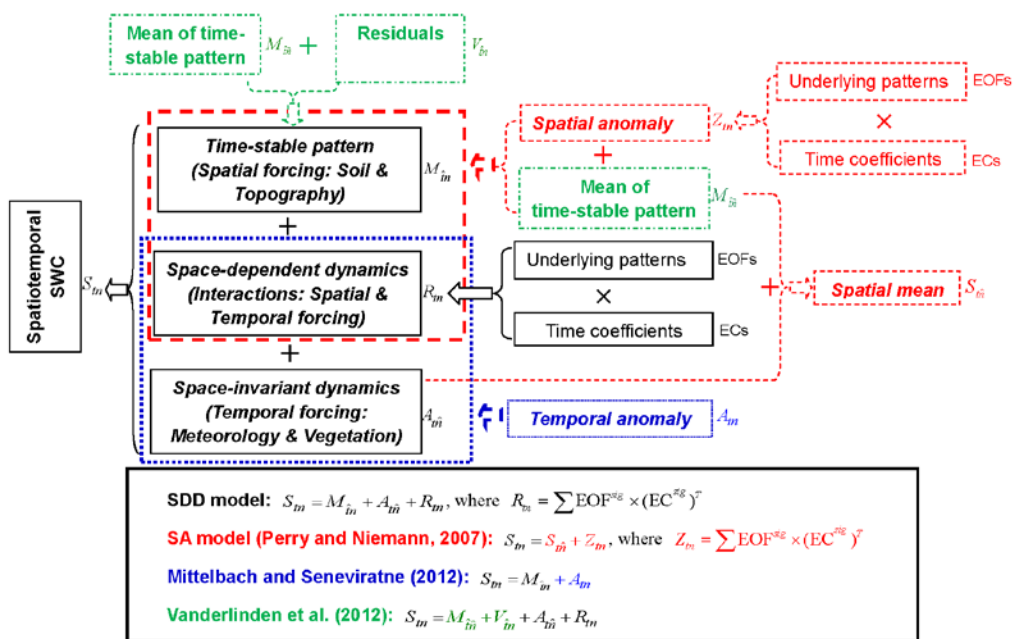


Fig. 1. Decomposition of spatiotemporal soil water content (SWC) in different models.

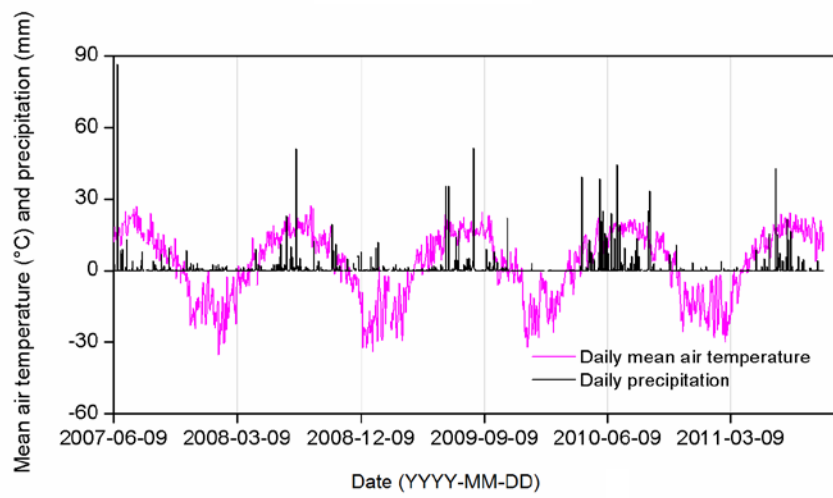


Fig. 2. Daily mean air temperature and precipitation during the study period.

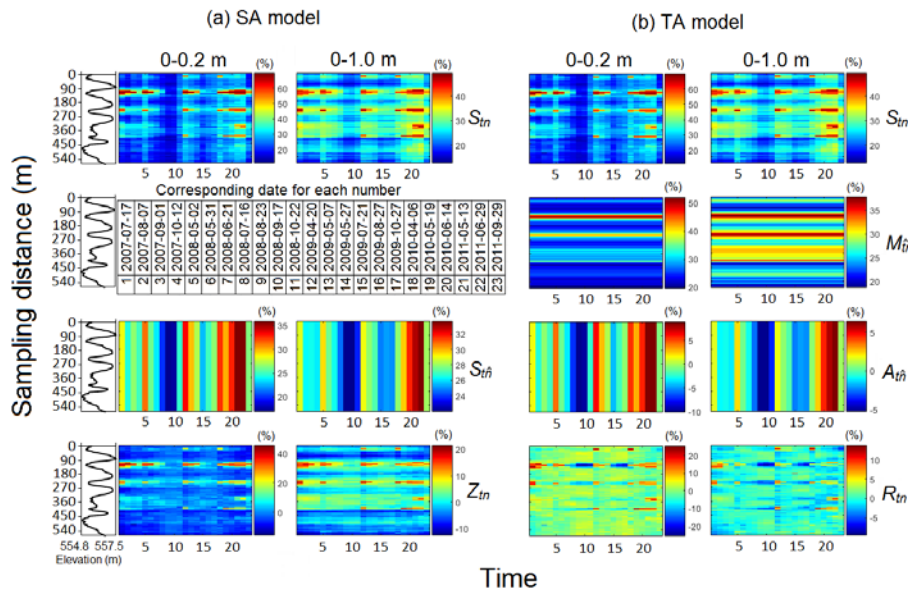


Fig. 3. Components of soil water content in (a) the SA model (spatial mean soil water content  $\hat{S}_{mn}$  and spatial anomaly  $\hat{Z}_{mn}$ ) and in (b) the TA model (time-stable pattern  $\hat{M}_{mn}$ , space-invariant temporal anomaly  $\hat{A}_{mn}$ , and space-variant temporal anomaly  $\hat{R}_{mn}$ ) for 0–0.2 and 0–1.0 m. Also shown is the elevation.



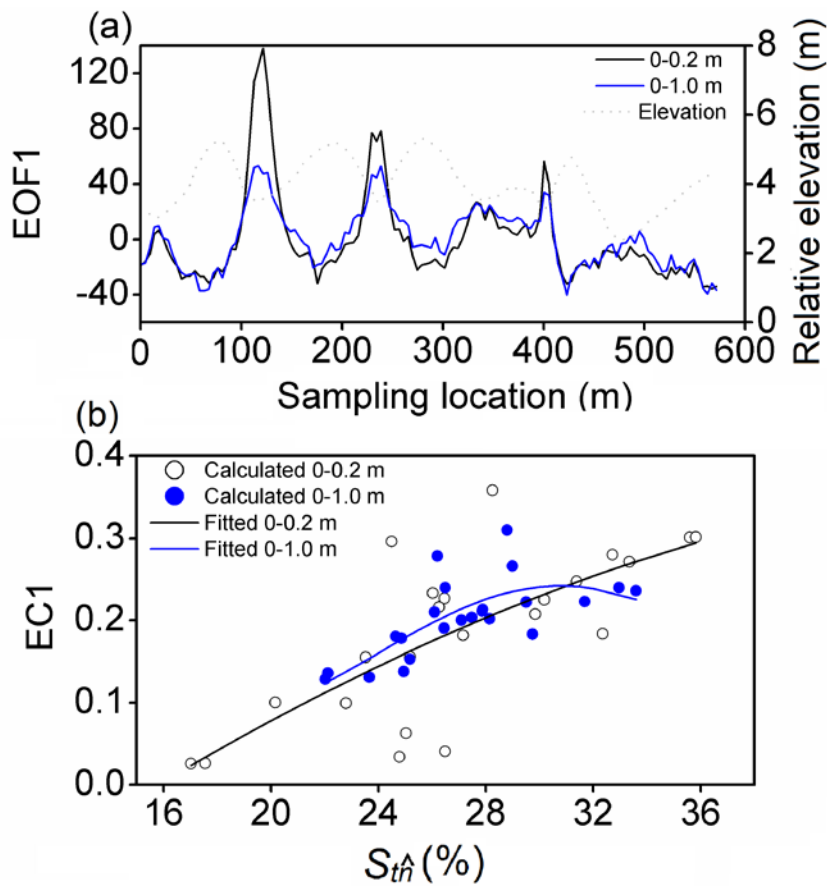


Fig. 4. (a) The EOF1 of the spatial anomaly  $Z_m$  and (b) relationships of associated EC1 versus spatial mean soil water content  $Z_m$  fitted by the cosine function (Eq. 4).

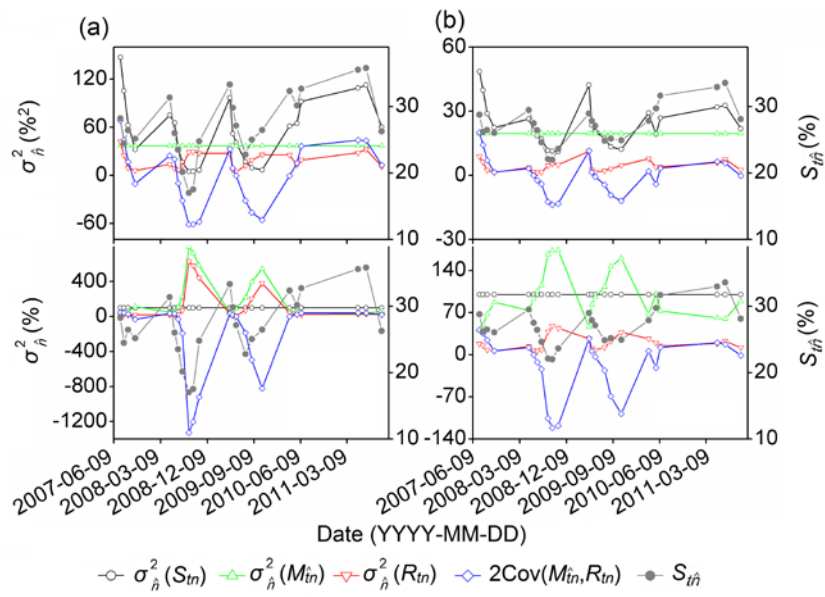


Fig. 5. Spatial variances of different components in Eq. (8) expressed in %<sup>2</sup> (upper panel) and as percentage (lower panel) for (a) 0–0.2 and (b) 0–1.0 m. Spatial mean soil water content  $S_{in}$  on each measurement day is also shown.

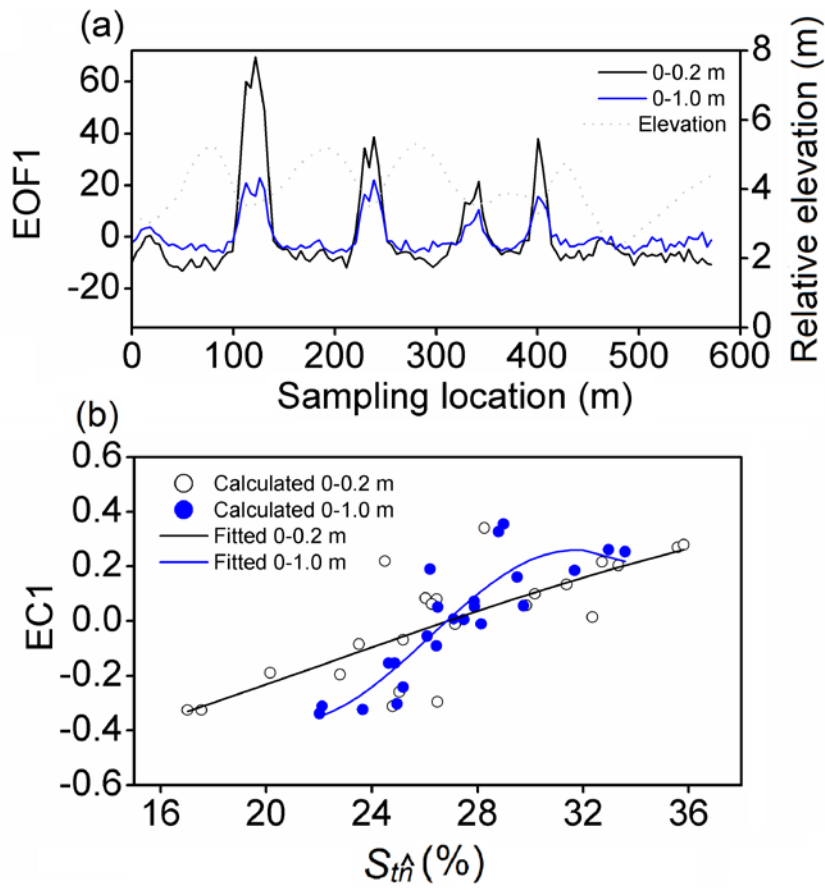


Fig. 6. (a) The EOF1 of the space-variant temporal anomaly  $R_{tn}$  and (b) relationships of associated EC1 versus spatial mean soil water content  $S_{\hat{n}}$  fitted by the cosine function (Eq. 4).

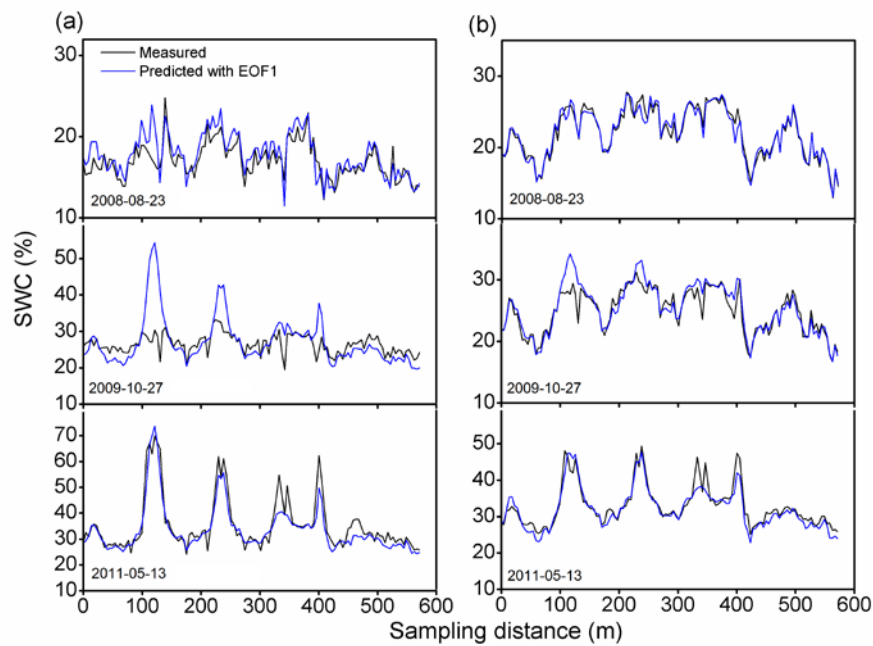


Fig. 7. Estimated soil water content (SWC) versus measured SWC for three dates at different soil water conditions (August 23, 2008, October 27, 2009, and May 13, 2011 are associated with relatively dry, medium, and wet days, respectively) using the TA model for (a) 0–0.2 and (b) 0–1.0 m.

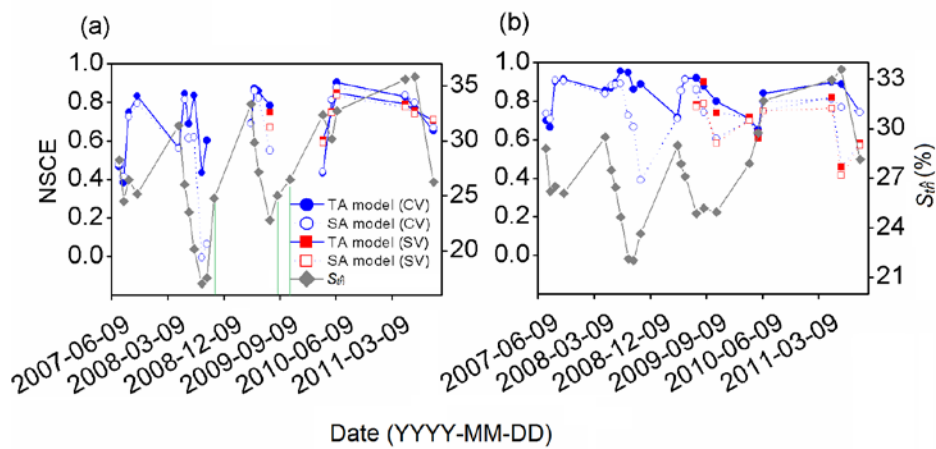
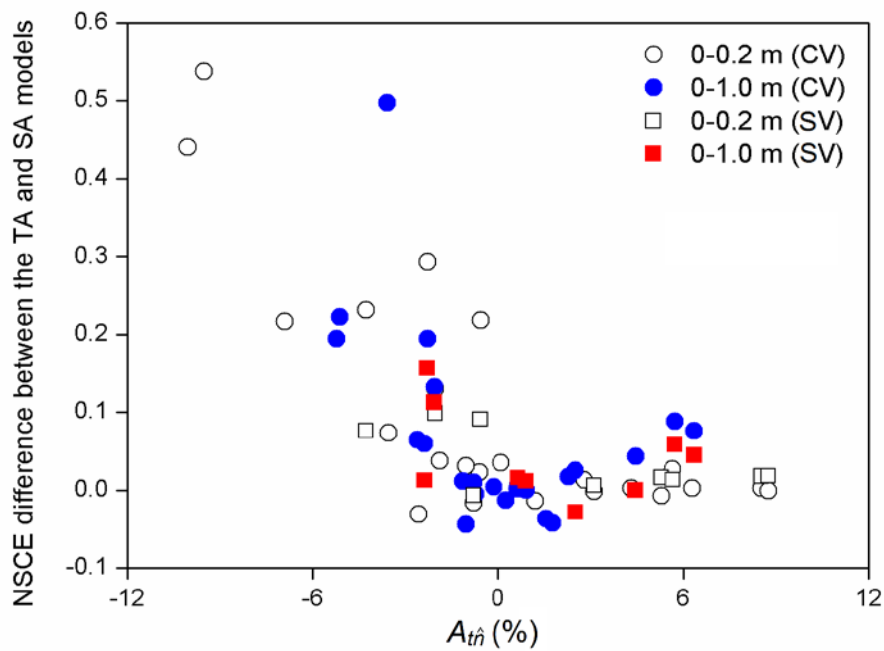


Fig. 8. The Nash-Sutcliffe coefficient of efficiency (NSCE) of soil water content estimation using the TA and SA models for (a) 0–0.2 and (b) 0–1.0 m for both cross validation (CV) and split sample external validation (SV). At 0–0.2 m, negative Nash-Sutcliffe coefficient of efficiency values for three dates (October 22, 2008, August 27, 2009, and October 27, 2009) as indicated by green lines present negative NSCE values (-4.05, -1.83, and -3.81, respectively, for the CV on the three dates; -2.63 and -5.12, respectively, for the SV on the latter two dates). are not shown.

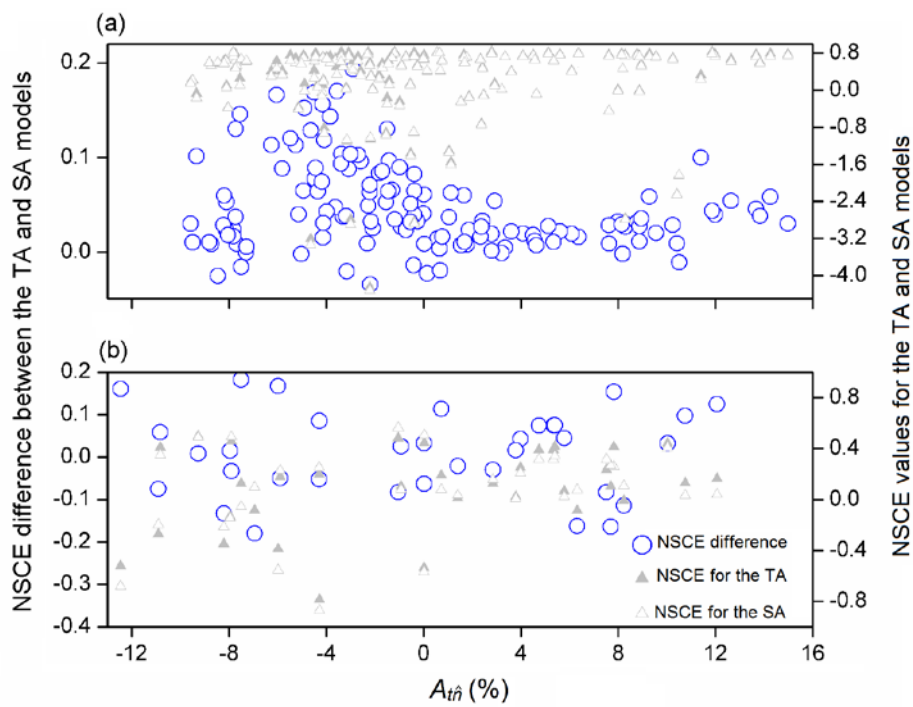
Spatial mean soil water content  $S_m$  on each measurement day is also shown.

Formatted: Font: (Default) Times New Roman, 12 pt, Font color: Text 1



Formatted: Font: (Default) Times New Roman, 12 pt, Font color: Text 1

Fig. 9. ~~Difference between the~~ Nash-Sutcliffe coefficient of efficiency (NSCE) ~~difference between the TA and SA models~~ of in terms of soil water content estimation ~~by using~~ both cross validation (CV) and ~~split sample external~~ validation (EVS) ~~using the TA and SA models~~ as a function of space-invariant temporal anomaly  $A_{t\hat{h}}$  for (a) 0–0.2 and (b) 0–1.0 m.



Formatted: Font: (Default) Times New Roman, 12 pt, Font color: Text 1

Fig. 10. Difference between the Nash-Sutcliffe coefficient of efficiency (NSCE) difference between the TA and SA models in terms of soil water content estimation using cross validation of soil water content evaluation by the cross validation using the TA and SA models as a function of space-invariant temporal anomaly  $A_{\hat{t}}$  for (a) 0–0.06 m of the Chinese Loess Plateau hillslope and (b) 0–0.15 m of the GENCAI network in Italy. The NSCE values for both models are also shown.